

Degrees-of-Freedom Region of MISO-OFDMA Broadcast Channel with Imperfect CSIT

Chenxi Hao, Borzoo Rassouli and Bruno Clerckx

Abstract

This contribution investigates the Degrees-of-Freedom region of a two-user frequency correlated Multiple-Input-Single-Output (MISO) Broadcast Channel (BC) with imperfect Channel State Information at the transmitter (CSIT). We assume that the system consists of an arbitrary number of subbands, denoted as L . Besides, the CSIT state varies across users and subbands. A tight outer-bound is found as a function of the minimum average CSIT quality between the two users. Based on the CSIT states across the subbands, the DoF region is interpreted as a weighted sum of the optimal DoF regions in the scenarios where the CSIT of both users are perfect, alternatively perfect and not known. Inspired by the weighted-sum interpretation and identifying the benefit of the optimal scheme for the unmatched CSIT proposed by Chen et al., we also design a scheme achieving the upper-bound for the general L -subband scenario in frequency domain BC, thus showing the optimality of the DoF region.

I. INTRODUCTION

Channel State Information at the Transmitter (CSIT) is crucial to the DoF performance in downlink Broadcast Channel, but having perfect CSIT is a challenging issue. In practice, each user estimates, quantizes and reports its CSI to the transmitter. This process is subject to imperfectness and latency. Their impact on the DoF region has attracted a lot of attention in recent years. The usefulness of the perfect but completely outdated CSIT was studied in [1]. Literature [2] generalized the findings in [1] by giving an optimal DoF region for an alternative CSIT setting, where the CSIT of each user can be perfect, delayed or none. Moreover, authors in [3], [4] and [5] looked into the scenario with both perfect delayed CSIT and imperfect instantaneous CSIT, whose qualities are shown to make an impact on the optimal DoF region. [6] and [7] extended the results of [3] and [5] by considering the different qualities of instantaneous CSIT of the two users. Furthermore, the authors of [8] studied the scenario where both delayed CSIT and instantaneous CSIT are imperfect and the results were generalized to a scenario with multiple slots and evolving CSIT states in [9]. Recently, all the results found in two-user time-correlated MISO BC with delayed CSIT have been extended to the MIMO case in [10]–[12]. Other works, such as [13]–[21] have covered other related topics about the DoF region of time domain BC.

However, in practical systems like Long Term Evolution (LTE), the system performance loss of Multiuser MIMO (MU-MIMO) is primarily due to CSI measurement and feedback inaccuracy rather than delay [22]. Therefore, assuming the CSI arrives at the transmitter instantaneously, we are interested in the frequency domain BC where the CSI is measured and reported to the transmitter on a per-subband basis. Due to frequency selectivity, constraints on uplink overhead and user distribution in the cell, the quality of CSI reported to the transmitter varies across users and subbands.

The alternating CSIT state ($I_{11}I_{12}=NP$ and $I_{21}I_{22}=PN$)¹ can be interpreted as two users reporting their CSI in two different subbands. Those unmatched CSIT was shown still useful in benefiting the DoF region in [2]. A sum DoF of $\frac{3}{2}$ is achieved, outperforming that in the case without CSIT. The scheme proposed in [2], called $S_3^{3/2}$, transmits two private symbols and one common message (to be decoded by both users) in two channel uses (subbands/slots). The key point lies in sending the common message twice in different subbands, so that the two users can decode it in turn due to the alternating CSIT in each subband. With the knowledge of the common message, the private symbols are recovered.

A more general scenario consists in having the channel state changing to $I_{11}I_{12}=\beta\alpha$ and $I_{21}I_{22}=\alpha\beta$ (where α and β represent the quality of the imperfect CSIT, both ranging from 0 to 1). Literature [23] was the first work investigating this issue. A novel transmission strategy integrating Maddah-Ali and Tse (MAT) scheme, ZFBF and FDMA was proposed. Recently, the DoF region found in [23] has been improved by the scheme proposed in [24], which combines $S_3^{3/2}$ scheme, ZFBF and FDMA. It outperforms [23] because no extra channel use is required to decode all the symbols. The DoF region in the alternating (α, β) scenario has been conversed in our conference paper [25]. The optimal DoF region was interpreted as a weighted sum of the DoF region in the CSIT state PP , PN/NP and NN . The weights are functions of the CSIT qualities of the two users, revealing an equivalence between the CSIT quality and the fraction of time when the CSIT is perfect as in [2].

Chenxi Hao, Borzoo Rassouli and Bruno Clerckx are with the Communication and Signal Processing group of Department of Electrical and Electronics, Imperial College London, email: chenxi.hao10;b.rassouli12;b.clerckx@imperial.ac.uk

This paper was in part published in "MISO Broadcast Channel with Imperfect and (Un)matched CSIT in the Frequency Domain: DoF Region and Transmission Strategies", PIMRC'13.

This work was supported in part by Samsung Electronics and by the Seventh Framework Programme for Research of the European Commission under grant number HARP-318489.

¹ I_{jk} is the CSIT state of user k in subband j . PP means perfect CSIT for both users; NN stands for no CSIT for both users; PN/NP refer to the CSIT states alternating between Perfect/None and None/Perfect.

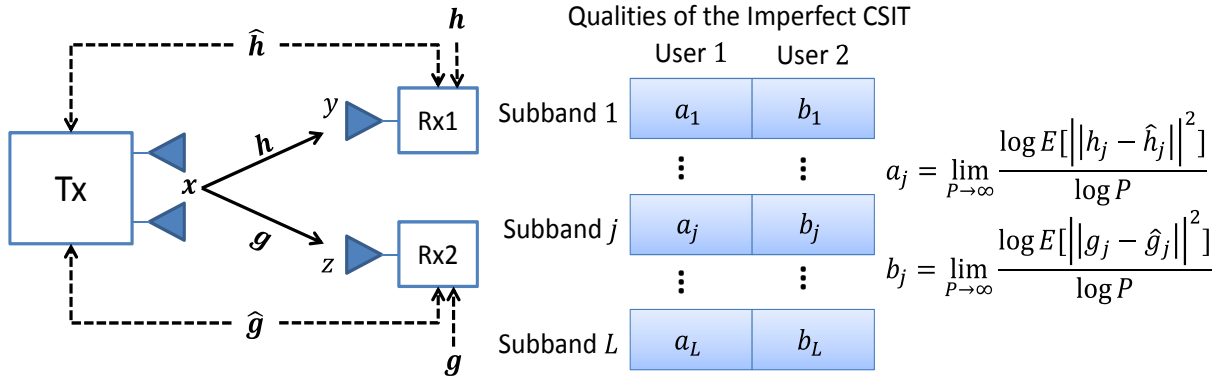


Fig. 1: System model of two-user MISO Broadcast Channel, with arbitrary values of the CSIT qualities across L subbands.

So far, the literature addressing the problem of frequency domain BC (or time domain BC without delayed CSIT) focuses on two subbands and assumes that the CSIT states alternate. This assumption is relatively optimistic as in a more realistic wireless communication framework two users may be scheduled simultaneously on multiple subbands. The channels in different subbands may have weak correlation due to the frequency selectivity. The qualities of the CSIT can also vary across users and subbands. We aim at understanding whether the multiple and arbitrary CSIT state can synergistically boost the *DoF* region. In this paper, we generalize our results of [25] to an L -subband scenario with arbitrary values of the CSIT qualities of both users (see Figure 1). In particular, we highlight the main contributions as follows:

- 1) We derive a tight outer-bound to the *DoF* region in the L -subband frequency correlated MISO BC with arbitrary values of CSIT qualities. It is shown to be a function of the minimum average CSIT quality between the two users. The converse relies on the upper-bound in [26], the extremal inequality [27] and Lemma 1 in [3].
- 2) The *DoF* region is interpreted as the weighted sum of the *DoF* region in the subchannels with state PP , PN/NP and NN , after we decompose the subbands into subchannels according to the qualities of the imperfect CSIT. The weights refer to the fraction of channel use of each type of the subchannels. For a given average CSIT quality but different distributions of the quality in each subband, we find the *DoF* region remains unchanged but the compositions of the region are varying. Besides, we find a similar expression of the *DoF* region as in [2], if we interpret the average CSIT quality as the fraction of channel use where the CSIT is perfect. This weighted-sum interpretation also provides an instructive insight into the achievable scheme.
- 3) By identifying the sub-optimality in the scheme proposed in [23] and the optimality of the scheme in [24] for a 2-subband scenario, we propose the optimal transmission strategy achieving the outer-bound of the *DoF* region in a 3-subband scenario with $\sum_{j=1}^3 a_j = \sum_{j=1}^3 b_j$ (a_j and b_j are the qualities of user 1 and user 2 respectively in subband j). Also, we extend this scheme to the L -subband scenario with $\sum_{j=1}^L a_j = \sum_{j=1}^L b_j$. The key point lies in generating multiple common messages and sending them twice such that the two users can recover them alternatively and decode the private symbols afterwards.
- 4) Following the footsteps of the construction of the optimal scheme in the case with $\sum_{j=1}^L a_j = \sum_{j=1}^L b_j$, we design an optimal transmission strategy for the L -subband scenario with $\sum_{j=1}^L a_j \neq \sum_{j=1}^L b_j$.

The rest of this paper is organized as follows. The system model is introduced in Section II, where the main results are also included. The converse of the *DoF* region is provided in Section III. A weighted-sum interpretation of the optimal *DoF* region is derived in Section IV. In Section V, by analyzing the achievability in the two-subband scenario, the optimal transmission strategy for L -subband with $\sum_{j=1}^L a_j = \sum_{j=1}^L b_j$ is designed. In Section VI, we build the transmission strategy for L -subband with $\sum_{j=1}^L a_j \neq \sum_{j=1}^L b_j$. Section VII concludes the paper.

The following notations are used throughout the paper. Bold lower case letters stand for vectors whereas a symbol not in bold font represents a scalar. $(\cdot)^T$ and $(\cdot)^H$ represent the transpose and conjugate transpose of a matrix or vector respectively. \mathbf{h}^\perp denotes the orthogonal space of the channel vector \mathbf{h} . $\mathcal{E}[\cdot]$ refers to the expectation of a random variable, vector or matrix. $\|\cdot\|$ is the norm of a vector. $A_{j_1}^{j_2}$ refers to the set $\{A_{j_1}, A_{j_1+1}, \dots, A_{j_2}\}$, if $j_1 \leq j_2$, otherwise $A_{j_1}^{j_2} = \emptyset$. $|A_{j_1}^{j_2}|$ represents the cardinality of set $A_{j_1}^{j_2}$, which equals to $j_2 - j_1$. If a is a scalar, $|a|$ is the absolute value of a . $f(P) \sim P^B$ corresponds to $\lim_{P \rightarrow \infty} \frac{\log f(P)}{\log P} = B$, where P is SNR throughout the paper and logarithms are in base 2.

II. SYSTEM MODEL AND MAIN RESULTS

A. Frequency domain two-user MISO BC

In this contribution, we consider a system as shown in Figure 1, which has a transmitter with two antennas and two users each with a single antenna. Denoting the transmit signal as \mathbf{x}_j subject to $E[\|\mathbf{x}_j\|^2] \leq P$, the observations at user 1 and 2, y_j

and z_j respectively, are given by

$$y_j = \mathbf{h}_j^H \mathbf{x}_j + \epsilon_{j1}, \quad (1)$$

$$z_j = \mathbf{g}_j^H \mathbf{x}_j + \epsilon_{j2}, \quad (2)$$

where $j \in [1, L]$. ϵ_{j1} and ϵ_{j2} are unit power AWGN noise. \mathbf{h}_j and \mathbf{g}_j , both with unit norm, are respectively the CSI of user 1 and user 2 in *subband* j . The CSI are i.i.d across users and subbands. In this contribution, the transmit signal can be made up of three kinds of messages:

- *Common message I*, denoted as c_j hereafter, is broadcast to both users in subband j . They should be recovered by both users, but can be intended exclusively for user 1 or user 2;
- *Common message II*, denoted as $u_0(\cdot)$ hereafter, should be recovered by both users, but can be intended exclusively for user 1 or user 2. Unlike c_j , $u_0(\cdot)$ is broadcast twice, i.e. once in the subbands where the quality of CSIT of user 1 is higher than that of user 2, and once in the subbands where the quality of CSIT of user 2 is higher than that of user 1;
- *Private message*, is intended for one user only, namely u_j for user 1 and v_j for user 2 in subband j .

B. CSI Feedback Model

Classically, in Frequency Division Duplexing (FDD), each user estimates their CSI in the specified subband using pilot and the estimated CSI is quantized and reported to the transmitter via a rate-limited link. In Time Division Duplexing (TDD), CSI is measured on the uplink and used in the downlink assuming channel reciprocity. We assume a general setup where the transmitter obtains the CSI instantaneously, but with imperfectness, due to the estimation error and/or finite rate in the feedback link.

Denoting $\hat{\mathbf{h}}_j$ and $\hat{\mathbf{g}}_j$ as the imperfect CSI of user 1 and user 2 in *subband* j respectively, the CSI of user 1 and user 2 can be respectively modeled as

$$\mathbf{h}_j = \hat{\mathbf{h}}_j + \tilde{\mathbf{h}}_j, \quad \mathbf{g}_j = \hat{\mathbf{g}}_j + \tilde{\mathbf{g}}_j, \quad j = 1 \cdots L, \quad (3)$$

where $\tilde{\mathbf{h}}_j$ and $\tilde{\mathbf{g}}_j$ are the corresponding error vectors, respectively with the covariance matrix $\mathbb{E}[\tilde{\mathbf{h}}_j \tilde{\mathbf{h}}_j^H] = \sigma_{j1}^2 \mathbf{I}_2$ and $\mathbb{E}[\tilde{\mathbf{g}}_j \tilde{\mathbf{g}}_j^H] = \sigma_{j2}^2 \mathbf{I}_2$. $\hat{\mathbf{h}}_j$ and $\hat{\mathbf{g}}_j$ are respectively independent of $\tilde{\mathbf{h}}_j$ and $\tilde{\mathbf{g}}_j$. The norm of $\hat{\mathbf{h}}_j$ and $\hat{\mathbf{g}}_j$ scale as P^0 at infinite SNR.

We employ the notation $\mathcal{S}_j \triangleq \{\mathbf{h}_j, \mathbf{g}_j\}$ to represent the CSI of both users in subband j . Similarly, $\hat{\mathcal{S}}_j \triangleq \{\hat{\mathbf{h}}_j, \hat{\mathbf{g}}_j\}$ is the set of the imperfect CSI, $\tilde{\mathcal{S}}_j \triangleq \{\tilde{\mathbf{h}}_j, \tilde{\mathbf{g}}_j\}$ refers to the set of the CSI errors and $\mathcal{S}_j = \{\hat{\mathcal{S}}_j, \tilde{\mathcal{S}}_j\}$. \mathcal{H}_1^n and \mathcal{H}_2^n respectively refer to sets of the imperfect CSI and the CSI error of user 1 while $\hat{\mathcal{G}}_1^n$ and $\hat{\mathcal{G}}_2^n$ are similarly defined. In addition, $\hat{\mathcal{S}}_1^n$ is available at both the transmitter side and the receiver side. \mathcal{H}_1^n and $\hat{\mathcal{G}}_1^n$ are only perfectly known by user 1 and user 2 respectively.

To investigate the impact of the imperfect CSIT on the *DoF* region, we assume that the variance of each entry in the error vector exponentially scales with SNR as in [3], [4], [6]–[12], [19], [21], [23]–[25], [28], namely $\sigma_{j1}^2 \sim P^{-a_j}$ and $\sigma_{j2}^2 \sim P^{-b_j}$. a_j and b_j are respectively interpreted as the quality of the CSIT of user 1 and user 2 in subband j , given as follows

$$a_j = \lim_{P \rightarrow \infty} -\frac{\log \sigma_{j1}^2}{\log P}, \quad b_j = \lim_{P \rightarrow \infty} -\frac{\log \sigma_{j2}^2}{\log P}. \quad (4)$$

a_j and b_j vary within the range of $[0, 1]$. $a_j = 1$ (resp. $b_j = 1$) is equivalent to perfect CSIT because the full *DoF* region can be achieved by simply doing ZFBF. $a_j = 0$ (resp. $b_j = 0$) is equivalent to no CSIT because it means that the variance of the CSI error scales as P^0 , such that the imperfect CSIT cannot benefit the *DoF* when doing ZFBF. Besides, a_j and b_j vary across all the L subbands. It is important to note the following quantities

$$\mathcal{E}[|\mathbf{h}_j^H \hat{\mathbf{h}}_j^\perp|^2] = \mathcal{E}[|(\hat{\mathbf{h}}_j + \tilde{\mathbf{h}}_j)^H \hat{\mathbf{h}}_j^\perp|^2] \quad (5)$$

$$= \mathcal{E}[|\tilde{\mathbf{h}}_j^H \hat{\mathbf{h}}_j^\perp|^2] \quad (6)$$

$$= \mathcal{E}[\tilde{\mathbf{h}}_j^H \hat{\mathbf{h}}_j^\perp \hat{\mathbf{h}}_j^\perp H \tilde{\mathbf{h}}_j] \sim P^{-a_j}. \quad (7)$$

as they are frequently used in the achievable schemes in Section V and VI. Similarly, we have $\mathcal{E}[|\mathbf{g}_j^H \hat{\mathbf{g}}_j^\perp|^2] \sim P^{-b_j}$.

It is worth noting that the CSIT pattern in Figure 1 is applicable to time domain. Specifically, the CSI report from each user arrives at the transmitter without latency, but it is imperfect due to the estimation error and/or finite rate in the feedback link. As the location of the users and their channel condition changes with time, the CSIT quality varies across users and transmission time-slots.

C. DoF Definition

Making use of the same notation as in [29] and [30], a rate pair (R_1, R_2) is said to be achievable in an L -subband BC with arbitrary imperfect CSIT qualities if there exists a code sequence $(2^{nR_1}, 2^{nR_2}, n)$ such that

- *Codebook construction*: There is one message set for each user. To be specific, M_1 for user 1 is uniformly distributed in the set $\mathcal{M}_1 \triangleq [1 : 2^{nR_1}]$ and M_2 , intended for user 2, is similarly distributed in the set $\mathcal{M}_2 \triangleq [1 : 2^{nR_2}]$.

- *Encoding*: The encoder randomly chooses a message M_1 from \mathcal{M}_1 and generate $u_1^n(M_1, \hat{\mathcal{S}}_1^n)$ according to the probability $\prod_{i=1}^n p(u_i|\hat{\mathcal{S}}_i)$. At the same time $v_1^n(M_2, \hat{\mathcal{S}}_1^n)$ with the probability $\prod_{i=1}^n p(v_i|\hat{\mathcal{S}}_i)$ is generated as a function of M_2 which is randomly chosen from \mathcal{M}_2 . Finally, the codeword $x_1^n(u_1^n, v_1^n, \hat{\mathcal{S}}_1^n)$ is generated with the probability $\prod_{i=1}^n p(x_i|u_i, v_i, \hat{\mathcal{S}}_1^n)$.
- *Decoding*: Receiver 1 wishes to decode M_1 and declares message $\hat{M}_1(y_1^n, \hat{\mathcal{S}}_1^n, \hat{\mathcal{S}}_1^n)$ is sent if it is the unique message such that y_1^n and $u_1^n(\hat{M}_1, \hat{\mathcal{S}}_1^n)$ are jointly typical. Similarly, receiver 2 declares message $\hat{M}_2(z_1^n, \hat{\mathcal{S}}_1^n, \hat{\mathcal{S}}_1^n)$ is sent if it is the unique message such that z_1^n and $v_1^n(\hat{M}_2, \hat{\mathcal{S}}_1^n)$ are jointly typical. Otherwise, an error $P_e^{(n)}$ will occur. By the Law of Large Numbers, we have $P_e^{(n)} \rightarrow 0$ when $n \rightarrow \infty$.

The capacity region, \mathcal{C} , is formed by all the achievable rate pairs. The DoF region, \mathcal{D} , is accordingly defined on a per-channel-use basis as follows

$$\mathcal{D} \triangleq \left\{ (d_1, d_2) \mid \forall (w_1, w_2) \in \mathbb{N}^2, \forall (R_1, R_2) \in \mathcal{C}, w_1 d_1 + w_2 d_2 \leq \limsup_{P \rightarrow \infty} \frac{w_1 R_1 + w_2 R_2}{r \log P} \right\}, \quad (8)$$

where r is the channel uses actually employed to achieve the rate pair (R_1, R_2) .

D. Problem Model

The average CSIT quality of user 1 and user 2 are respectively expressed as $a_e = \frac{1}{L} \sum_{j=1}^L a_j$ and $b_e = \frac{1}{L} \sum_{j=1}^L b_j$. Without the loss of generality, in the rest of this paper, we consider $a_j \geq b_j$ in subband 1 to l ($l \leq L$) and $a_j \leq b_j$ for the remaining subbands. For convenience, we denote $q_j^+ \triangleq a_j - b_j$ if $a_j \geq b_j$ (namely for $j \leq l$) while $q_j^- \triangleq b_j - a_j$ if $a_j \leq b_j$ (namely for $l+1 \leq j \leq L$). Then, we have $\{q^+\} \triangleq \{q_1^+, q_2^+, \dots, q_l^+\}$ and $\{q^-\} \triangleq \{q_{l+1}^-, q_{l+2}^-, \dots, q_L^-\}$.

For any positive integer L , we define two classes of problems as follows

Definition 1. \mathcal{P}_L Problem: Achieve the optimal DoF region in a scenario such that $a_e = b_e$.

Definition 2. \mathcal{Q}_L Problem: Achieve the optimal DoF region in a scenario such that $a_e \neq b_e$. Note that for $a_e > b_e$ (resp. $a_e < b_e$), it is called \mathcal{Q}_L^+ (resp. \mathcal{Q}_L^-) Problem hereafter.

A \mathcal{P}_L problem considers the general L -subband scenario with $a_e = b_e$. Specifically, if there exists a subset of the subbands, denoted as \mathcal{J} , such that $\sum_{j_1 \in \mathcal{J}} a_{j_1} = \sum_{j_1 \in \mathcal{J}} b_{j_1}$, the \mathcal{P}_L problem can be solved as a combination of a $\mathcal{P}_{|\mathcal{J}|}$ and a $\mathcal{P}_{L-|\mathcal{J}|}$ problems. If no such subset \mathcal{J} is found, the \mathcal{P}_L problem considers the most complicated L -subband scenario with $a_e = b_e$. For instance, when $L=2$ and $a_1 + a_2 = b_1 + b_2$, there generally exist two possible CSIT patterns: 1) $a_1 = b_1$ and $a_2 = b_2$; 2) $a_1 \neq b_1$ and $a_2 \neq b_2$. The first case refers to two \mathcal{P}_1 problems and the optimal scheme is obtained by performing the solution to \mathcal{P}_1 problem twice (separately and independently in subband 1 and 2). However, for the second case, the transmitted signal in each subband is correlated to each other (see Section V-B). Similarly, a \mathcal{Q}_L^+ problem considers the general L -subband scenario with $a_e > b_e$. In other words, for a \mathcal{P}_L and a \mathcal{Q}_L^+ problem, the transmitted signals vary according the actual CSIT quality pattern (formed by the frequency-user grid as shown in Figure 1). More details of the achievabilities in a \mathcal{P}_L problem and a \mathcal{Q}_L^+ are shown in Section V and VI respectively.

E. Main Results

Theorem 1. The optimal DoF region, \mathcal{D} , in a L -subband frequency correlated BC with imperfect varying CSIT is specified by

$$d_1 + d_2 \leq 1 + \frac{1}{L} \min \left(\sum_{j=1}^L a_j, \sum_{j=1}^L b_j \right), \quad (9)$$

$$d_1 \leq 1, \quad (10)$$

$$d_2 \leq 1, \quad (11)$$

where a_j and b_j are respectively the quality of the CSIT of user 1 and user 2 in subband j and L can be any integer values.

Note that the optimal DoF region is bounded by the minimum average CSIT quality between user 1 and user 2. This result gives an affirmative answer to the conjecture in [2] that the sum DoF is 1 in a two-user MISO BC with fixed PN CSIT state. The converse is provided in Section III. The achievability is discussed in Section V and VI, for \mathcal{P}_L ($a_e = b_e$) and \mathcal{Q}_L ($a_e \neq b_e$) problem respectively. The following corollary provides an instructive insight into the formation of the optimal DoF region.

Corollary 1. The optimal DoF region in the frequency correlated BC with imperfect CSIT can be interpreted as a weighted sum of three basis optimal DoF regions

$$\mathcal{D} = \frac{1}{L} (\bar{r}\bar{\mathcal{D}} + \hat{r}\hat{\mathcal{D}} + \tilde{r}\tilde{\mathcal{D}}), \quad (12)$$

where $\bar{\mathcal{D}}$, $\hat{\mathcal{D}}$ and $\tilde{\mathcal{D}}$ refer to the optimal DoF region for a CSIT state of PP, PN/NP and NN respectively and \bar{r} , \hat{r} and \tilde{r} are the corresponding weights, given as

$$\bar{\mathcal{D}}: d_1 \leq 1, d_2 \leq 1, \quad (13)$$

$$\hat{\mathcal{D}}: d_1 + d_2 \leq \frac{3}{2}, d_1 \leq 1, d_2 \leq 1, \quad (14)$$

$$\tilde{\mathcal{D}}: d_1 + d_2 \leq 1, \quad (15)$$

$$\bar{r} = \sum_{j=1}^L \min(a_j, b_j), \quad (16)$$

$$\hat{r} = 2 \min\left(\sum_{j=1}^l q_j^+, \sum_{j=l+1}^L q_j^-\right), \quad (17)$$

$$\tilde{r} = L - \bar{r} - \hat{r}. \quad (18)$$

III. CONVERSE OF THEOREM 1

The objective of this section is to provide the converse of Theorem 1. Before going into the details, we highlight the key ingredients in the derivation as

- Nair-Gamal bound [26]: provides an upper-bound to the DoF region in a general BC;
- Extremal Inequality: maximizes a weighted difference of two different entropies;
- Lemma 1 in [3]: upper- and lower-bound the entropy.

Let us revisit the converse in previous works. In [15], the DoF region in the BC without CSIT is upper-bounded by considering one user's observation is degraded compared to the other's. In the BC with delayed CSIT [1] [3] [5], the outer-bound is obtained through the genie-aided model where one user's observation is provided to the other, thus establishing a physically degraded BC to remove the delayed CSIT.

However, in this contribution, those methods are not adopted since the transmitter does not have delayed CSIT and the BC with imperfect CSIT cannot be simply considered as a degraded BC. Instead, we follow the assumption in [31]: We first consider that user 2 knows the message intended for user 1, which leads to an outer-bound denoted by \mathbb{D}_1 ; Then by assuming that user 1 knows user 2's desired message, we can have another region \mathbb{D}_2 . The final DoF outer-bound results from the intersection of them, i.e. $\mathbb{D} = \mathbb{D}_1 \cap \mathbb{D}_2$. This assumption is consistent with the derivation in Korner-Marton bound (Theorem 5 and Appendix I in [32]) and Nair-Gamal bound (Theorem 2.1 and 3.1 in [26], proof given in the Appendix of Lecture Notes 9 in [30]). Both of these two bounds provide an outer-bound to the general discrete memoryless broadcast channel and Nair-Gamal bound is said to be in general contained in Korner-Marton bound [26]. As a consequence, we aim at finding the following bounds

$$R_1 + R_2 \leq I(U; Y|V) + I(V; Z), \quad (19)$$

$$R_1 + R_2 \leq I(U; Y) + I(V; Z|U). \quad (20)$$

The key challenge lies in finding the auxiliary variables U and V .

Assuming user 2 has the knowledge of M_1 and according to Fano's Inequality, we have

$$nR_1 \leq I(M_1; Y_1^n | \hat{\mathcal{S}}_1^n, \tilde{\mathcal{H}}_1^n) \quad (21)$$

$$= I(M_1; Y_1^n | \hat{\mathcal{S}}_1^n, \tilde{\mathcal{H}}_1^n, \tilde{\mathcal{G}}_1^n) \quad (22)$$

$$nR_2 \leq I(M_2; Z_1^n | M_1, \hat{\mathcal{S}}_1^n, \tilde{\mathcal{G}}_1^n) \quad (23)$$

$$= I(M_2; Z_1^n | M_1, \hat{\mathcal{S}}_1^n, \tilde{\mathcal{G}}_1^n, \tilde{\mathcal{H}}_1^n) \quad (24)$$

$$n(R_1 + R_2) \leq I(M_1; Y_1^n | \hat{\mathcal{S}}_1^n, \tilde{\mathcal{H}}_1^n, \tilde{\mathcal{G}}_1^n) + I(M_2; Z_1^n | M_1, \hat{\mathcal{S}}_1^n, \tilde{\mathcal{G}}_1^n, \tilde{\mathcal{H}}_1^n) \quad (25)$$

$$= I(M_1; Y_1^n | \mathcal{S}) + I(M_2; Z_1^n | M_1, \mathcal{S}), \quad (26)$$

where (22) follows the fact that $Y_1^n \rightarrow \{\hat{\mathcal{S}}_1^n, \tilde{\mathcal{H}}_1^n\} \rightarrow \tilde{\mathcal{G}}_1^n$ forms a Markov chain such that Y_1^n is independent of $\tilde{\mathcal{G}}_1^n$ conditioned on $\{\hat{\mathcal{S}}_1^n, \tilde{\mathcal{H}}_1^n\}$. (24) follows similarly. In (26), $\{\hat{\mathcal{S}}_1^n, \tilde{\mathcal{G}}_1^n, \tilde{\mathcal{H}}_1^n\}$ is replaced by \mathcal{S} . (26) is bounded by

$$n(R_1 + R_2) \leq \sum_{j=1}^n \{I(M_1, Y_1^{j-1}, Z_{j+1}^n, \hat{\mathcal{S}}_1^n; Y_j | \mathcal{S}_1^n) + I(M_2, Y_1^{j-1}, Z_{j+1}^n, \hat{\mathcal{S}}_1^n; Z_j | M_1, \mathcal{S}_1^n, Y_1^{j-1}, Z_{j+1}^n)\} \quad (27)$$

$$= \sum_{j=1}^n \{I(U_j; Y_j | \mathcal{S}_1^n) + I(V_j; Z_j | U_j, \mathcal{S}_1^n)\}. \quad (28)$$

The derivation of (27) is provided in the Appendix. Now, we have found the auxiliary variables as

$$U_j \triangleq \{M_1, Y_1^{j-1}, Z_{j+1}^n, \hat{\mathcal{S}}_1^n\}, \quad (29)$$

$$V_j \triangleq \{M_2, Y_1^{j-1}, Z_{j+1}^n, \hat{\mathcal{S}}_1^n\}. \quad (30)$$

Continuing deriving (28), we have

$$n(R_1 + R_2) \leq \sum_{j=1}^n \underbrace{h(Y_j | \mathcal{S}_1^n)}_{\leq \log P} - h(Y_j | \mathcal{S}_1^n, U_j) + h(Z_j | \mathcal{S}_1^n, U_j) - \underbrace{h(Z_j | \mathcal{S}_1^n, U_j, V_j)}_{\leq o(\log P)} \quad (31)$$

$$\leq n \log P + \sum_{j=1}^n \{h(Z_j | \mathcal{S}_1^n, U_j) - h(Y_j | \mathcal{S}_1^n, U_j)\}. \quad (32)$$

Next, we focus on the terms in the summation of (32) and upper-bound them using a similar derivation as in [3]. For convenience, we give up the index j . Consequently,

$$h(Z | \mathcal{S}, U) - h(Y | \mathcal{S}, U) \leq \max_{P_U P_{\mathbf{x}|U}} \{h(Z | U, \mathcal{S}) - h(Y | U, \mathcal{S})\} \quad (33)$$

$$\leq \max_{P_U} \mathcal{E}_U \{ \max_{P_{\mathbf{x}|U}} h(Z | U = U^*, \mathcal{S}) - h(Y | U = U^*, \mathcal{S}) \} \quad (34)$$

$$\leq \max_{P_U} \mathcal{E}_U \{ \max_{P_{\mathbf{x}|U}} \mathcal{E}_{\mathcal{S}|U} [h(Z | U = U^*, \mathcal{S} = \mathcal{S}^*) - h(Y | U = U^*, \mathcal{S} = \mathcal{S}^*)] \} \quad (35)$$

$$= \max_{P_U} \mathcal{E}_U \{ \max_{P_{\mathbf{x}|U}} \mathcal{E}_{\mathcal{S}|\hat{\mathcal{S}}} [h(\mathbf{g}^H \mathbf{x} + \epsilon_2 | U = U^*) - h(\mathbf{h}^H \mathbf{x} + \epsilon_1 | U = U^*)] \} \quad (36)$$

$$\leq \max_{P_U} \mathcal{E}_U \{ \max_{\mathbf{0} \preceq \mathbf{C}, \text{tr}(\mathbf{C}) \leq P} \max_{\substack{P_{\mathbf{x}|U} \\ \text{Cov}(\mathbf{x}|U) \preceq \mathbf{C}}} \mathcal{E}_{\mathcal{S}|\hat{\mathcal{S}}} [h(\mathbf{g}^H \mathbf{x} + \epsilon_2 | U = U^*) - h(\mathbf{h}^H \mathbf{x} + \epsilon_1 | U = U^*)] \} \quad (37)$$

$$\leq \max_{P_U} \mathcal{E}_U \{ \max_{\mathbf{0} \preceq \mathbf{C}, \text{tr}(\mathbf{C}) \leq P} \mathcal{E}_{\mathcal{S}|\hat{\mathcal{S}}} [\log(1 + \mathbf{g}^H \mathbf{K} \mathbf{g}) - \log(1 + \mathbf{h}^H \mathbf{K} \mathbf{h})] \}, \quad (38)$$

$$\leq \mathcal{E}_{\hat{\mathcal{S}}} \{ \max_{\mathbf{0} \preceq \mathbf{K}, \text{tr}(\mathbf{K}) \leq P} \mathcal{E}_{\mathcal{S}|\hat{\mathcal{S}}} [\log(1 + \mathbf{g}^H \mathbf{K} \mathbf{g}) - \log(1 + \mathbf{h}^H \mathbf{K} \mathbf{h})] \}, \quad (39)$$

where \mathbf{K} is the covariance matrix of \mathbf{x} (i.e. $\text{Cov}(\mathbf{x}|U) = \mathbf{K}$) and \mathbf{C} is a semi-definite matrix, which is regarded as the constraint of \mathbf{K} . (38) is derived according to the fact 1) $\mathbf{x} \rightarrow U \rightarrow \mathcal{S}$ forms a Markov chain so that \mathcal{S} is independent of \mathbf{x} conditioned on U ; 2) With a constrained covariance, a Gaussian distributed \mathbf{x} conditioned on U is the optimal solution to the maximization of the weighted difference in (38) for any positive semi-definite \mathbf{C} , based on the proof of Corollary 6 in [27].

Using Lemma 1 in [3], we can respectively upper- and lower-bound the first and second terms in (39) as

$$\mathcal{E}_{\mathcal{S}|\hat{\mathcal{S}}} \log(1 + \mathbf{g}^H \mathbf{K} \mathbf{g}) \leq \log(1 + \lambda_1 \mathcal{E}[\|\tilde{\mathbf{g}}\|^2]) + o(1), \quad (40)$$

$$\mathcal{E}_{\mathcal{S}|\hat{\mathcal{S}}} \log(1 + \mathbf{h}^H \mathbf{K} \mathbf{h}) \geq \log(1 + e^{-\gamma} \lambda_1 \mathcal{E}[\|\tilde{\mathbf{h}}\|^2]) + o(1), \quad (41)$$

where γ is a constant, λ_1 is the largest eigen-value of the covariance matrix \mathbf{K} . Substituting the terms in (39) with (40) and (41), we can have the j th term in the summation of (32) upper-bounded by

$$h(Z_j | \mathcal{S}_1^n, U_j) - h(Y_j | \mathcal{S}_1^n, U_j) \leq \log \frac{1 + \lambda_1 \mathcal{E}[\|\tilde{\mathbf{g}}_j\|^2]}{1 + e^{-\gamma} \lambda_1 \mathcal{E}[\|\tilde{\mathbf{h}}_j\|^2]} \quad (42)$$

$$\approx a_j \log P. \quad (43)$$

Applying (43) to all the terms in (32), the sum rate is upper-bounded by

$$n(R_1 + R_2) \leq n \log P + \sum_{j=1}^n a_j \log P \quad (44)$$

$$R_1 + R_2 \leq \log P + \frac{1}{n} \sum_{j=1}^n a_j \log P. \quad (45)$$

When n tends to infinity, the L -subband scenario defined in Figure 1 repeats infinite times. Consequently, the CSIT state in each subband appears $n \times \frac{1}{L}$ times and (45) can be rewritten as

$$R_1 + R_2 \leq \log P + \frac{1}{n} \sum_{j=1}^L \frac{n}{L} a_j \log P = \log P + \frac{1}{L} \sum_{j=1}^L a_j \log P, \quad (46)$$

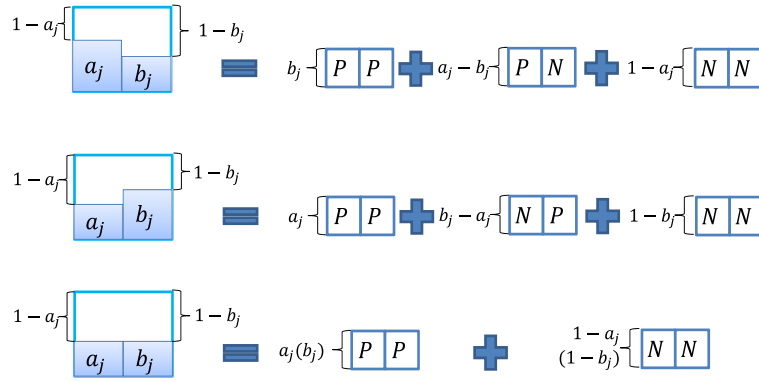


Fig. 2: Subband j is decomposed to subchannels with states PP , NP/PN and NN , each with an amount of channel use determined according to the CSIT qualities.

Accordingly, the DoF region is specified as follows

$$\mathbb{D}_1 : d_1 + d_2 \leq 1 + a_e = 1 + \frac{\sum_{j=1}^L a_j}{L}. \quad (47)$$

Switching the role of each user results in the sum rate and DoF region specified as

$$n(R_1 + R_2) \leq \sum_{j=1}^n \{I(U_j; Y_j | \mathcal{S}_1^n, V_j) + I(V_j; Z_j | \mathcal{S}_1^n)\} \quad (48)$$

$$\leq n \log P + \sum_{j=1}^n h(Y_j | \mathcal{S}_1^n, V_j) - h(Z_j | \mathcal{S}_1^n, V_j) \quad (49)$$

$$\leq n \log P + \sum_{j=1}^n b_j \log P, \quad (50)$$

$$R_1 + R_2 \leq \log P + \frac{1}{L} \sum_{j=1}^L b_j \log P, \quad (51)$$

$$\mathbb{D}_2 : d_1 + d_2 \leq 1 + b_e = 1 + \frac{\sum_{j=1}^L b_j}{L}. \quad (52)$$

Taking the intersection of \mathbb{D}_1 and \mathbb{D}_2 results in (9). Together with the single-user constraint, Theorem 1 holds. \square

IV. A WEIGHTED-SUM INTERPRETATION OF THE OPTIMAL DoF REGION

In this section, we provide an insight into the formation of the optimal DoF region. According to the particular CSIT setting, each subband is considered as composed of three parallel subchannels with different fraction of channel use. The DoF region of each subchannel has been found in previous work. We will show that the optimal DoF region stated in Theorem 1 can be calculated as a weighted sum of the DoF region of each subchannel.

A. Intuition: Channel Decomposition

In this part, we decompose the channel in each subband following the intuition that the imperfect CSIT with error variance $P^{-\alpha}$ can be considered as perfect for α ($0 \leq \alpha \leq 1$) channel use (i.e. the transmit power is reduced to $\mathcal{E}[\|s\|^2] \leq P^\alpha$). We can see this by simply sending one private message per user using ZFBF precoding and with power P^α . Since $\mathcal{E}[\|\mathbf{h}_j^H \hat{\mathbf{h}}_j^\perp\|] \sim P^{-\alpha}$ and $\mathcal{E}[\|\mathbf{g}_j^H \hat{\mathbf{g}}_j^\perp\|] \sim P^{-\alpha}$, both users can recover their private messages subject to noise. Therefore, the rate $\alpha \log P$ is achieved per user. As only α channel has been used, full DoF region (i.e. $d_1=1$ and $d_2=1$) is obtained according to (8). This is in fact a generalization of the fact that full DoF region can be obtained if the variance of CSIT error is scaled as SNR^{-1} [3].

Consequently, a subband j with the CSIT error scaling as P^{-a_j} and P^{-b_j} for user 1 and 2 respectively, is decomposed as shown in Figure 2. The transmitter is assumed to have perfect knowledge of the CSI of user 1 for a_j channel use while for the remaining $1-a_j$ channel use, no CSIT of user 1 is available. The same approach is employed for user 2. It results three subchannels, each of which can be interpreted using the same notation as in [2] (NN , PN/NP and PP).

- \tilde{j} : NN channel, no CSIT of either user, with channel use $1 - \max(a_j, b_j)$;

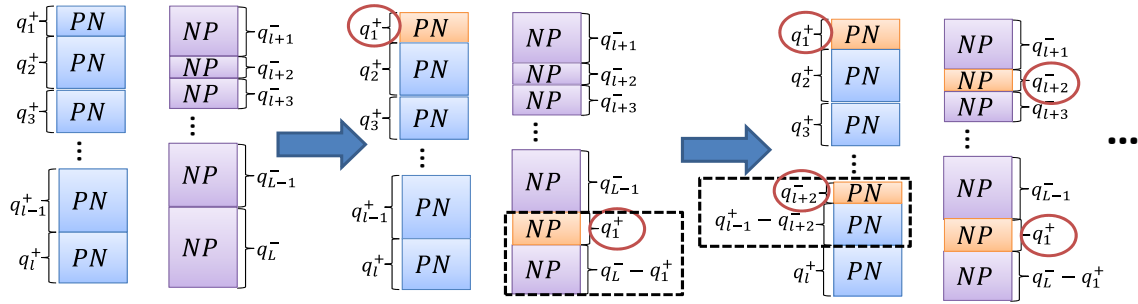


Fig. 3: An example of further decomposing subchannel \hat{j} to have multiple equivalent alternating PN/NP scenario.

- \hat{j} : PN (resp. NP) channel, perfect CSIT of user 1 (resp. 2) but no CSIT of use 2 (resp. 1), with channel use q_j^+ (resp. q_j^-);
- \bar{j} : PP channel, perfect CSIT of both users, with channel use $\min(a_j, b_j)$.

In this way, the original L -subband scenario becomes the product of those parallel subchannels. The DoF region is obtained as the weighted-sum of that in each subchannel.

B. DoF Regions of the Subchannels

We split the rate of each user into three parts, namely $R_1 = \tilde{R}_1 + \hat{R}_1 + \bar{R}_1$ and $R_2 = \tilde{R}_2 + \hat{R}_2 + \bar{R}_2$, where $(\tilde{R}_1, \tilde{R}_2)$ represents the rate pair achieved in the subchannel with state NN , (\hat{R}_1, \hat{R}_2) refers to the rate pair achieved in the subchannel with alternating PN/NP state while (\bar{R}_1, \bar{R}_2) is the rate pair achieved in the subchannel with state PP . The message intended to user 1 and 2 is therefore generated from a set jointly formed by $\tilde{\mathcal{M}}_1 \times \hat{\mathcal{M}}_1 \times \bar{\mathcal{M}}_1 = [1:2^{n\tilde{R}_1}][1:2^{n\hat{R}_1}][1:2^{n\bar{R}_1}]$ and $\tilde{\mathcal{M}}_2 \times \hat{\mathcal{M}}_2 \times \bar{\mathcal{M}}_2 = [1:2^{n\tilde{R}_2}][1:2^{n\hat{R}_2}][1:2^{n\bar{R}_2}]$ respectively. The subsets $(\tilde{\mathcal{M}}_k, \hat{\mathcal{M}}_k, \bar{\mathcal{M}}_k)$ are independent of each other for $k=1,2$. $(\tilde{R}_1, \tilde{R}_2)$, (\hat{R}_1, \hat{R}_2) and (\bar{R}_1, \bar{R}_2) respectively result in the DoF region $\tilde{\mathcal{D}}$, $\hat{\mathcal{D}}$ and $\bar{\mathcal{D}}$.

1) *Subchannel \bar{j}* : When the transmitter has perfect CSI of both users, the optimal DoF region is expressed as follows

$$\bar{\mathcal{D}} : d_1 \leq 1, d_2 \leq 1, \quad (53)$$

which can be achieved via ZFBF. The total amount of channel use of the subchannels with PP state is

$$\bar{r} = \sum_{j=1}^L \min(a_j, b_j). \quad (54)$$

2) *Subchannel \hat{j}* : In this class of subchannels, the transmitter has perfect knowledge of the CSI of user 1 or (exclusive) user 2. As a reminder, we assume $a_j \geq b_j$ in subband 1 to l ($l \leq L$) and $a_j \leq b_j$ for the remaining subbands. Following the way where channels are decomposed (as in Figure 2), there are in total l PN subchannels, each with channel use $q_j^+ = a_j - b_j, j \leq l$ and $L-l$ NP subchannels, each with channel use $q_j^- = b_j - a_j, l+1 \leq j \leq L$. Literature [2] provides an optimal DoF region of the alternating PN/NP scenario, which can be achieved by the simple $S_3^{3/2}$ scheme. This bound is denoted by $\hat{\mathcal{D}}$ and expressed as

$$\hat{\mathcal{D}} : d_1 + d_2 \leq \frac{3}{2}, d_1 \leq 1, d_2 \leq 1. \quad (55)$$

However, this region is optimal for the alternating PN/NP scenario where each PN and NP subchannel have the same amount of channel use, namely $\forall j_1 \in [1, l], \exists j_2 \in [l+1, L]$ such that $q_{j_1}^+ = q_{j_2}^-$. In a general L -subband scenario (Definition 1 and 2), this condition does not necessarily hold. Hence, we aim at showing that (55) still optimally bounds the DoF region of the PN and NP subchannels. To that end, we further decompose the subchannels in order to find the alternating PN/NP scenario.

Figure 3 shows an example of the further decomposition. Firstly, subchannel \hat{L} is decomposed into two NP subchannels, namely $\hat{L}(1)$ and $\hat{L}(2)$, respectively with fraction of channel use q_1^+ and $q_L^- - q_1^+$. In this way, subchannel $\hat{1}$ and $\hat{L}(1)$ form an alternating PN/NP scenario where PN and NP states have equal amount of channel use. Secondly, subchannel $\hat{l-1}$ is decomposed into two PN subchannels, namely $(\hat{l-1})(1)$ and $(\hat{l-1})(2)$, respectively with fraction of channel use q_{l+2}^- and $q_{l-1}^+ - q_{l+2}^-$. Then we consider subchannel $(\hat{l-1})(1)$ and $\hat{l+2}$ as an alternating PN/NP scenario. Such process can be repeated till no PN subchannels or NP subchannels remains. Consequently, multiple alternating PN/NP scenario are found, with the total amount of channel use (denoted as \hat{r})

$$\hat{r} = 2 \min\left(\sum_{j=1}^l q_j^+, \sum_{j=l+1}^L q_j^-\right). \quad (56)$$

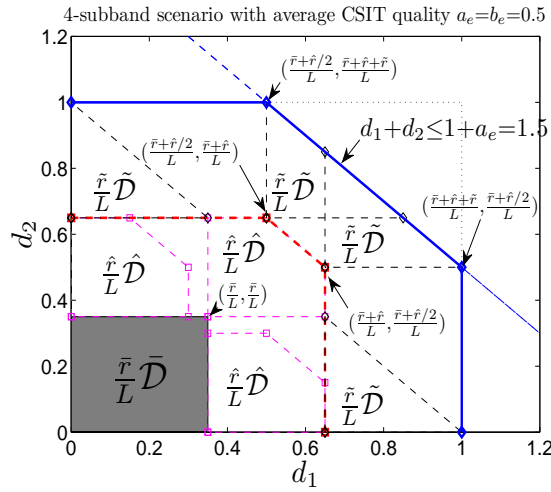


Fig. 4: The composition of the optimal DoF of a 4-subband scenario, with $(a_1, b_1) = (0.7, 0.3)$, $(a_2, b_2) = (0.6, 0.4)$, $(a_3, b_3) = (0.4, 0.7)$ and $(a_4, b_4) = (0.3, 0.6)$, thus $(a_e, b_e) = (0.5, 0.5)$.

When $\sum_{j=1}^l q_j^+ \neq \sum_{j=l+1}^L q_j^-$, for instance a \mathcal{Q}_L problem, the remaining $\hat{r}' = |\sum_{j=1}^l q_j^+ - \sum_{j=l+1}^L q_j^-|$ channel use of PN (or NP) subchannels are merged with the subchannels with state NN . This is because the DoF region of a PN (or NP) subchannel is identical to that of a NN subchannel, according to Theorem 1 applied to the case where $a_{1:L} = 1$ and $b_{1:L} = 0$.

3) *Subchannel \tilde{j}* : In subchannel \tilde{j} , the transmitter has no knowledge of the CSI of both users. The optimal DoF region (denoted as $\tilde{\mathcal{D}}$) has been studied in [13] and [15], which can be achieved by simply performing FDMA. This optimal DoF region writes as

$$\tilde{\mathcal{D}} : d_1 + d_2 \leq 1. \quad (57)$$

Subband \tilde{j} have $L - \sum_{j=1}^L \max(a_j, b_j)$ channel use in total. Combining with the \hat{r}' channel use of PN (or NP) subchannels, the total amount of channel use where $\hat{\mathcal{D}}$ is optimal is

$$\tilde{r} = L - \sum_{j=1}^L \max(a_j, b_j) + \hat{r}'. \quad (58)$$

C. Weighted-Sum

As the rate per user can be expressed as $R_k = \frac{1}{L}(\bar{r}\bar{R}_k + \hat{r}\hat{R}_k + \tilde{r}\tilde{R}_k)$, we interpret the optimal DoF region as

$$\begin{aligned} \mathcal{D} &= \frac{1}{L}(\bar{r}\bar{\mathcal{D}} + \hat{r}\hat{\mathcal{D}} + \tilde{r}\tilde{\mathcal{D}}) \\ &= \frac{\sum_{j=1}^L \min(a_j, b_j)}{L} \bar{\mathcal{D}} + \frac{2\min(\sum_{j=l+1}^L q_j^-, \sum_{j=1}^l q_j^+)}{L} \hat{\mathcal{D}} + \frac{L - \sum_{j=1}^L \max(a_j, b_j) + |\sum_{j=1}^l q_j^+ - \sum_{j=l+1}^L q_j^-|}{L} \tilde{\mathcal{D}}, \end{aligned} \quad (59)$$

Figure 4 illustrates the composition of \mathcal{D} . The grey square area depicts the region $\frac{\bar{r}}{L}\bar{\mathcal{D}}$, specified by the corner point $(\frac{\bar{r}}{L}, \frac{\bar{r}}{L})$. All the valid points inside $\frac{\bar{r}}{L}\bar{\mathcal{D}}$ are expanded to a magenta polygon representing $\frac{\hat{r}}{L}\hat{\mathcal{D}}$. This expansion results in the bound shown in the dashed red curve with square points, outlined by the corner points $(\frac{\bar{r}+\hat{r}/2}{L}, \frac{\bar{r}+\hat{r}}{L})$ and $(\frac{\bar{r}+\hat{r}}{L}, \frac{\bar{r}+\hat{r}/2}{L})$. Then, every point on this bound is further expanded to a black triangle area referring to the DoF region $\frac{\tilde{r}}{L}\tilde{\mathcal{D}}$. Outlining all the expanded area, we can obtain \mathcal{D} specified by the solid blue curve with diamond points $(\frac{\bar{r}+\hat{r}/2}{L}, \frac{\bar{r}+\hat{r}+\tilde{r}}{L})$ and $(\frac{\bar{r}+\hat{r}+\tilde{r}}{L}, \frac{\bar{r}+\hat{r}/2}{L})$. Replacing \bar{r} , \hat{r} and \tilde{r} with (54), (56) and (58) respectively, we interpret the diamond points as (assuming $\sum_{j=1}^l q_j^+ > \sum_{j=l+1}^L q_j^-$, i.e. $\sum_{j=1}^L a_j > \sum_{j=1}^L b_j$ without loss of generality)

$$\bar{r} + \hat{r} + \tilde{r} = L, \quad (60)$$

$$\bar{r} + \hat{r}/2 = \sum_{j=1}^L \min(a_j, b_j) + \sum_{j=l+1}^L q_j^- \quad (61)$$

$$= \sum_{j=1}^L b_j = \min(\sum_{j=1}^L a_j, \sum_{j=1}^L b_j), \quad (62)$$

showing that the corner points are lying on the boundary of inequalities (9), (10) and (11).

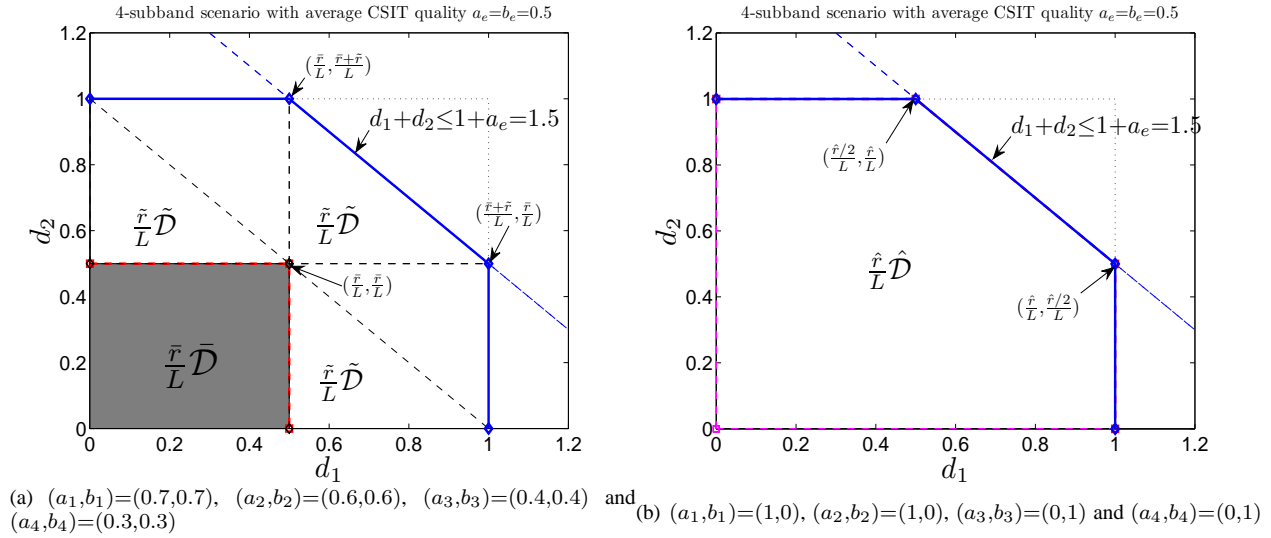


Fig. 5: The composition of the optimal DoF of a 4-subband scenario, with $(a_e, b_e) = (0.5, 0.5)$.

Remark 1. [Equivalence with Remark 1 in [2]]

According to (62), the optimal DoF region can be rewritten as

$$\mathcal{D}: \quad d_1 + d_2 \leq 1 + \frac{1}{L} \min\left(\sum_{j=1}^L a_j, \sum_{j=1}^L b_j\right) = 1 + \frac{\bar{r} + \hat{r}}{L}. \quad (63)$$

As we have respectively interpreted the weight \bar{r} , \hat{r} and \tilde{r} in (59) as the fraction of the subchannels with state PP, NP/PN and NN, $\frac{\bar{r} + \hat{r}}{L}$ in (63) in fact stands for the fraction of channel use where the CSIT of a single user is perfect. Revisiting Remark 1 in [2], the sum DoF is bounded by

$$d_1 + d_2 \leq 1 + \lambda_P + \lambda_D, \quad (64)$$

where λ_P (resp. λ_D) refers to the fraction of time where the CSIT of a single user is perfect (resp. delayed). When $\lambda_D = 0$, (64) becomes a function of λ_P . Through the weighted-sum interpretation, (63) bridges Theorem 1 in this contribution and Remark 1 in [2] and find the equivalence between a_e (assuming $a_e = b_e$) and λ_P . Moreover, the upper-bound of the sum DoF in (9) generalizes (64) when $\lambda_D = 0$, because the CSIT states in [2], namely PN, NP, NN and PP, are particular cases of the system model investigated in this paper.

Remark 2. [The composition of the DoF region changes with CSIT profile]

Figure 5(a) and 5(b) illustrate the formation of the optimal DoF region of a 4-subband scenario, with identical average CSIT quality as in Figure 4 (i.e. $a_e = b_e = 0.5$, $L = 4$), but different profile of the CSIT qualities.

Specifically, in Figure 5(a), the transmitter has the knowledge of each user's CSI with the same quality in each subband. The channels are decomposed into subchannels with PP and NN states. The optimal DoF region is therefore a function of only $\tilde{\mathcal{D}}$ and $\tilde{\tilde{\mathcal{D}}}$. On the other hand, Figure 5(b) presents an alternating CSIT scenario, whose optimal DoF region is composed of only $\hat{\mathcal{D}}$.

Nonetheless, both of these two CSIT settings result in the same DoF region as that in Figure 4. Specifically, in Figure 5(a), $\bar{r} = \sum_{j=1}^4 a_j = 2$ and $\tilde{r} = L - \bar{r} = 2$, thus the corner points are $(\frac{1}{2}, 1)$ and $(1, \frac{1}{2})$. While in Figure 5(b), $\hat{r} = L$ leads to corner points $(\frac{1}{2}, 1)$ and $(1, \frac{1}{2})$. Hence, it is worth noting that if the average CSIT quality per user is fixed, the distribution of the CSIT qualities among the subbands only impacts the composition of the DoF region, but does not change the shape.

Remark 3. [Relationship between the composition and optimal scheme]

Since ZFBF, $S_3^{3/2}$ and FDMA are respectively the optimal schemes for the subchannels with state PP, PN/NP and NN (as mentioned in Section IV-B), the composition of the DoF region gives some insights into the optimal transmission scheme.

In Figure 5(a), the four subbands are decomposed into subchannels with PP and NN state. The optimality of the DoF region is achieved via a scheme integrating ZFBF and FDMA as studied in [25]. A similar phenomenon can be observed in Figure 5(b). The four subbands merely consists of the subchannels with PN/NP state, whose optimal DoF region $\hat{\mathcal{D}}$ composes $\tilde{\mathcal{D}}$ alone. Simply reusing $S_3^{3/2}$ scheme twice (i.e. in subband 1,2 and subband 3,4), the optimal DoF region is achieved.

Moreover, for a scenario with $L = 2$, $a_1 = b_1 = \beta$ and $a_2 = b_2 = \alpha$, the subbands are decomposed into PP, PN/NP and NN subchannels with $\bar{r} = 2\alpha$, $\hat{r} = 2(\beta - \alpha)$ and $\tilde{r} = 2(1 - \beta)$ channel use respectively (using (54), (56) and (58)). The optimal

subband 1	Power	Rate (logP)	subband 2	Power	Rate (logP)
c_1	$P-P^{a_1}$	$1-a_1$	c_2	$P-P^{b_2}$	$1-b_2$
u_1	$P^{b_1}/2$	b_1	u_2	$P^{b_2}/2$	b_2
u_0	$(P^{a_1} - P^{b_1})/2$	a_1-b_1	u_0	$(P^{b_2} - P^{a_2})/2$	b_2-a_2
v_1	$P^{a_1}/2$	a_1	v_2	$P^{a_2}/2$	a_2

TABLE I: Power and rate allocation in the optimal scheme for \mathcal{P}_2 problem.

DoF region is achieved via a scheme integrating ZFBF, $S_3^{3/2}$ scheme and FDMA, which is proposed in [24]. Intuitively, the composition of the optimal DoF region provides insights into the optimal transmission strategy.

V. ACHIEVABILITY OF \mathcal{P}_L PROBLEM

In this section, we will discuss the achievability of the optimal DoF region for the \mathcal{P}_L problem. We start with evaluating the schemes proposed in [23], [24] and [25] which investigated a 2-subband scenario with unmatched CSIT (namely $a_1=b_2=\beta$ and $a_2=b_1=\alpha$) and matched CSIT (namely, $a_1=b_1=\beta$ and $a_2=b_2=\alpha$). By identifying the key ingredients inside the schemes, the optimal scheme for the \mathcal{P}_L problem is found.

A. \mathcal{P}_1 Problem

In [25], a two-subband scenario with matched CSIT (namely $a_1=b_1=\beta$ and $a_2=b_2=\alpha$) is studied. As the CSIT quality of each user in each subband is equal to each other ($a_j=b_j$), the scenario with matched CSIT can be regarded as two parallel \mathcal{P}_1 problems. Reusing the transmission scheme introduced in [25], the optimal DoF region can be achieved. For a \mathcal{P}_1 problem, the optimal scheme transmits the signal in each subband by superposing a common message I with ZFBF-precoded private messages and writes as

$$\mathbf{x}_1 = \underbrace{[c_1, 0]^T}_{P-P^{a_1}} + \underbrace{\hat{\mathbf{g}}_1^\perp u_1}_{P^{a_1}/2} + \underbrace{\hat{\mathbf{h}}_1^\perp v_1}_{P^{a_1}/2}, \quad (65)$$

where c_1 is the common message broadcast to both users and u_1 and v_1 are symbols intended for user 1 and user 2 respectively.

The received signal at each user is expressed as

$$y_1 = \underbrace{h_{11}^* c_1}_P + \underbrace{\mathbf{h}_1^H \hat{\mathbf{g}}_1^\perp u_1}_{P^{a_1}/2} + \underbrace{\mathbf{h}_1^H \hat{\mathbf{h}}_1^\perp v_1}_{P^0} + \underbrace{\epsilon_{11}}_{P^0}, \quad z_1 = \underbrace{g_{11}^* c_1}_P + \underbrace{\mathbf{g}_1^H \hat{\mathbf{g}}_1^\perp u_1}_{P^0} + \underbrace{\mathbf{g}_1^H \hat{\mathbf{h}}_1^\perp v_1}_{P^{a_1}/2} + \underbrace{\epsilon_{12}}_{P^0}, \quad (66)$$

where the private symbols u_1 and v_1 are drowned by the noise respectively at user 2 and user 1 due to partial ZFBF. Both users decode the common message I first with rate $(1-a_1)\log P$ by treating the private message as noise. Afterwards using Successive Interference Cancellation (SIC), each user can decode their private message with rate $a_1\log P$ only subject to noise, after removing the common message. The DoF pairs $(1, a_1)$ and $(a_1, 1)$ are achieved if we consider the common message is intended for user 1 and user 2 respectively.

B. \mathcal{P}_2 Problem

As mentioned in Section II-D, a \mathcal{P}_2 problem considers two basic CSIT quality patterns: 1) $a_1=b_1$ and $a_2=b_2$; 2) $a_1 \neq b_1$ and $a_2 \neq b_2$. The first case is termed as the 2-subband scenario with matched CSIT, which consists of two parallel \mathcal{P}_1 problems. The achievability has been discussed in Section V-A. For the second CSIT quality pattern, the \mathcal{P}_2 problem can be considered as the scenario with unmatched CSIT, whose achievable DoF region has been investigated in [23] and [24]. As a reminder, we will identify the shortness of the scheme in [23] and the benefit of the optimal scheme in [24] through discussion and analysis.

1) *Optimal Scheme*: The optimal transmission blocks in *subband 1* and *2* are expressed as

$$\mathbf{x}_1 = [c_1, 0]^T + \hat{\mathbf{g}}_1^\perp u_1 + [u_0, 0]^T + \hat{\mathbf{h}}_1^\perp v_1, \quad (67)$$

$$\mathbf{x}_2 = [c_2, 0]^T + \hat{\mathbf{h}}_2^\perp v_2 + [u_0, 0]^T + \hat{\mathbf{g}}_2^\perp u_2. \quad (68)$$

Common message II, u_0 , and common messages I, c_1 and c_2 should be decoded by both users (but could be intended for user 1 and user 2 respectively or exclusively for user 1 or user 2). Note that we do not precode common messages I and II in this paper as it does not impact the DoF. u_1 and u_2 are symbols intended for user 1, while v_1 and v_2 are symbols intended for

user 2. The rate and power allocation are shown in Table I, resulting in the following received signals at each user

$$y_1 = \underbrace{h_{11}^* c_1}_P + \underbrace{\mathbf{h}_1^H \hat{\mathbf{g}}_1^\perp u_1}_{P^{b_1}} + \underbrace{h_{11}^* u_0}_{P^{a_1}} + \underbrace{\mathbf{h}_1^H \hat{\mathbf{h}}_1^\perp v_1}_{P^0} + \epsilon_{11}, \quad (69)$$

$$z_1 = \underbrace{g_{11}^* c_1}_P + \underbrace{\mathbf{g}_1^H \hat{\mathbf{g}}_1^\perp u_1}_{P^0} + \underbrace{g_{11}^* u_0}_{P^{a_1}} + \underbrace{\mathbf{g}_1^H \hat{\mathbf{h}}_1^\perp v_1}_{P^{b_1}} + \epsilon_{12}, \quad (70)$$

$$y_2 = \underbrace{h_{21}^* c_2}_P + \underbrace{\mathbf{h}_2^H \hat{\mathbf{g}}_2^\perp u_2}_{P^{b_2}} + \underbrace{h_{21}^* u_0}_{P^{b_2}} + \underbrace{\mathbf{h}_2^H \hat{\mathbf{h}}_2^\perp v_2}_{P^0} + \epsilon_{21}, \quad (71)$$

$$z_2 = \underbrace{g_{21}^* c_2}_P + \underbrace{\mathbf{g}_2^H \hat{\mathbf{g}}_2^\perp u_2}_{P^0} + \underbrace{g_{21}^* u_0}_{P^{b_2}} + \underbrace{\mathbf{g}_2^H \hat{\mathbf{h}}_2^\perp v_2}_{P^{a_2}} + \epsilon_{22}. \quad (72)$$

In (69), (70) and (71), (72), c_1 and c_2 are respectively decoded first by treating all the other terms as noise. Afterwards, user 1 decodes u_0 and u_1 from y_1 using SIC. With the knowledge of u_0 , u_2 can be recovered from y_2 . Similarly, user 2 decodes u_0 and v_2 from z_2 via SIC. v_1 can be decoded from z_1 by eliminating u_0 .

To keep the same notation as in [23]–[25], we replace a_1, b_2 with β and a_2, b_1 with α and $\beta \geq \alpha$. The *DoF* pair $(1, \frac{\alpha+\beta}{2}) = (1, \frac{\alpha+\beta}{2})$ and $(\frac{\alpha+\beta}{2}, 1) = (\frac{\alpha+\beta}{2}, 1)$ are achieved if we consider the common messages are intended for user 1 and user 2 respectively, consistent with the optimal *DoF* region. Note that when $\beta = \alpha$, the \mathcal{P}_2 problem will degrade to two parallel \mathcal{P}_1 problems and no common message Π , u_0 , is generated.

2) *Shortness of the Scheme Proposed in [23]*: In order to identify the shortness of the suboptimal scheme, we keep the same notation as in [23]–[25], namely $a_1 = b_2 = \beta$ and $a_2 = b_1 = \alpha$ and $\beta \geq \alpha$. In the suboptimal scheme, the transmit signals in subband 1 and 2 are respectively expressed as

$$\mathbf{x}_1 = [c_1, 0]^T + [\mu_1, 0]^T + [\hat{\mathbf{h}}_1^\perp, \hat{\mathbf{h}}_1][v_{11}, v_{12}]^T + \hat{\mathbf{g}}_1^\perp u_1, \quad (73)$$

$$\mathbf{x}_2 = [c_2, 0]^T + [\mu_2, 0]^T + [\hat{\mathbf{g}}_2^\perp, \hat{\mathbf{g}}_2][u_{21}, u_{22}]^T + \hat{\mathbf{h}}_2^\perp v_2, \quad (74)$$

where the private symbols u_1 , v_{11} , u_{21} and v_2 are precoded and transmitted with the power and rate similar to u_1 , v_1 , u_2 and v_2 in (67) and (68) respectively.

Besides, v_{12} and u_{22} , generated with rate $(\beta - \alpha) \log P$, are respectively overheard by user 1 in subband 1 and by user 2 in subband 2, thus leading to the requirement of transmitting $\mu = v_{12} + u_{22}$ to enable the decoding of other private symbols. μ is further split into μ_1 and μ_2 and multicast via an extra $\beta - \alpha$ channel use. However, no extra channel use is required in the optimal scheme, because u_0 is sent twice (i.e. subband 1 and 2) so that each user can decode it alternatively.

To sum up, the scheme in [23] employs $2\beta + \beta - \alpha$ channel use to transmit six private symbols (i.e. v_{11} , v_{12} , u_1 , u_{21} , u_{22} , v_2), while the optimal scheme sends five symbols (i.e. u_1 , v_2 , u_0 , v_1 , u_2) in 2β channel use. Besides, the common messages, c_1 and c_2 , are sent using $\max(2 - 3\beta + \alpha, 0)$ and $2 - 2\beta$ channel use in the sub-optimal and optimal scheme respectively. Their sum *DoF* are respectively expressed as

$$d_\Sigma^{sub} = \frac{2\beta + 2\alpha + 2(\beta - \alpha) + \max(2 - 3\beta + \alpha, 0)}{3\beta - \alpha + \max(2 - 3\beta + \alpha, 0)} \quad (75)$$

$$= \frac{4\alpha + 4(\beta - \alpha) + \max(2 - 3\beta + \alpha, 0)}{2\alpha + 3(\beta - \alpha) + \max(2 - 3\beta + \alpha, 0)}, \quad (76)$$

$$d_\Sigma^{opt} = \frac{2\beta + 2\alpha + (\beta - \alpha) + 2 - 2\beta}{2\beta + 2 - 2\beta} \quad (77)$$

$$= \frac{4\alpha + 3(\beta - \alpha) + 2 - 2\beta}{2\alpha + 2(\beta - \alpha) + 2 - 2\beta}. \quad (78)$$

Remark 4. [Shortness of the suboptimal scheme]

The sum *DoF* performance is further derived as (76) and (78), which provide an explicit interpretation of the sub-optimality of [23]. More precisely, with the weighted-sum interpretation, the denominator and numerator in each equation are written as the sum of three parts. Specifically, in (78), 2α channel use is employed by ZFBF and $4\alpha \log P$ sum rate (namely the rate of u_1 , v_2 and part of the rate of u_2 and v_1) is achieved; $S_3^{3/2}$ scheme performs on $2(\beta - \alpha)$ channel use and achieves $3(\beta - \alpha) \log P$ sum rate (namely the rate of u_0 and part of the rate of u_2 and v_1); The common messages, c_1 and c_2 , are sent via FDMA with $2 - 2\beta$ channel use.

However, as in (76), the scheme in [23] combines ZFBF, MAT and FDMA. 2α channel use is employed by ZFBF and $4\alpha \log P$ sum rate (namely the rate of u_1 , v_2 and part of the rate of u_{21} and v_{11}) is achieved; MAT scheme performs on $3(\beta - \alpha)$ channel use and achieves $4(\beta - \alpha) \log P$ sum rate (namely the rate of v_{12} and u_{22} and part of the rate of u_{21} and v_{11}). Compared to $S_3^{3/2}$, MAT scheme employs an extra $\beta - \alpha$ channel use, but only results in $\beta - \alpha$ rate improvement. At the same time, the fraction of FDMA transmission (namely, c_j) is shrunk to $2 - 3\beta + \alpha$. A *DoF* loss is incurred when $2 - 3\beta + \alpha < 0$,

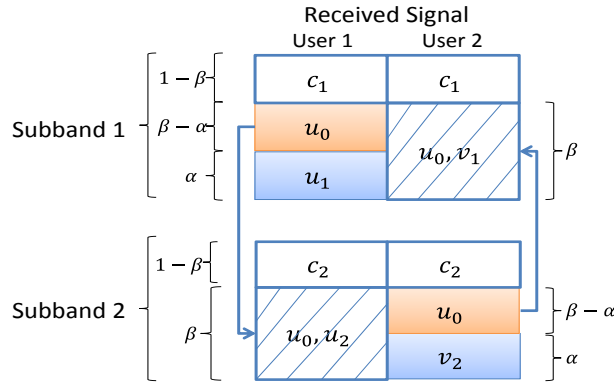


Fig. 6: The illustration of the received signal and decoding procedure of the optimal scheme for the \mathcal{P}_2 problem with $a_1=b_2=\beta$, $a_2=b_1=\alpha$ and $\beta \geq \alpha$, where the values beside the the bracket stand for the (pre-log factor of the) rate of the corresponding symbols. User 1 (resp. user 2) observes u_0 with higher power than u_1 (resp. v_2) in subband 1 (resp. 2) and receives u_0 with the same power level as u_2 (resp. v_1) in subband 2 (resp. 1). The common message u_0 can be decoded by both users but in different subbands. Then each user employs it to eliminate the interference and decode the private symbols.

	Power	Rate ($\log P$)		Power	Rate ($\log P$)		Power	Rate ($\log P$)
c_1	$P-P^{a_1}$	$1-a_1$	c_2	$P-P^{a_2}$	$1-a_2$	c_3	$P-P^{b_3}$	$1-b_3$
u_1	$P^{b_1}/2$	b_1	u_2	$P^{b_2}/2$	b_2	u_3	$P^{b_3}/2$	b_3
v_1	$P^{a_1}/2$	a_1	v_2	$P^{a_2}/2$	a_2	v_3	$P^{a_3}/2$	a_3
$u_0(1)$	$P^{a_1}/2-P^{b_1}/2$	a_1-b_1	$u_0(2)$	$P^{a_2}/2-P^{b_2}/2$	a_2-b_2	$u_0(1)$	$P^{b_3-q_2^+}/2-P^{a_3}/2$	$q_1^+=a_1-b_1$
						$u_0(2)$	$P^{b_3}/2-P^{b_3-q_2^+}/2$	$q_2^+=b_2-a_2$

TABLE II: Power and rate allocation in the optimal scheme for 3-subband case.

because the transmission of μ_1 and μ_2 (requiring an extra $\beta-\alpha$ channel use) cannot be completed using the remaining channel use (after generating the private symbols, which is $2-2\beta$) in subband 1 and 2.

Remark 5. [Key point in the optimal scheme]

Figure 6 provides an illustrative description of the received signals and decoding procedure of the optimal scheme. The key point to boost the DoF lies in making both users decode u_0 without the employment of any extra channel use. To this end, the transmitter broadcasts u_0 twice, i.e. subband 1 and 2. In subband 1, user 1 is said to be more capable to decode u_0 because it receives u_0 with a higher power than the private symbol u_1 . Similarly, user 2 is more capable in subband 2. In this way, both users can decode u_0 alternatively when they are more capable and no extra channel use is required.

As we will see in the following two subsections, this insight can be generalized to solve $\mathcal{P}_L, L \geq 3$ problem by generating multiple streams of u_0 and sending each of them twice. One is in subband $j_1 \in [1:l]$ and the other is in subband $j_2 \in [l+1, L]$, where user 1 and user 2 are respectively more capable to decode u_0 .

C. \mathcal{P}_3 Problem

In this part, we investigate a \mathcal{P}_3 problem ($\sum_{j=1}^3 a_j = \sum_{j=1}^3 b_j$) with $a_1 \geq b_1$, $a_2 \geq b_2$, $a_3 \leq b_3$ without the loss of generality. Inspired by Remark 5, we construct the optimal transmission block as follows

$$\mathbf{x}_1 = [c_1, 0]^T + \hat{\mathbf{g}}_1^\perp u_1 + [u_0(1), 0]^T + \hat{\mathbf{h}}_1^\perp v_1, \quad (79)$$

$$\mathbf{x}_2 = [c_2, 0]^T + \hat{\mathbf{g}}_2^\perp u_2 + [u_0(2), 0]^T + \hat{\mathbf{h}}_2^\perp v_2, \quad (80)$$

$$\mathbf{x}_3 = [c_3, 0]^T + \hat{\mathbf{g}}_3^\perp u_3 + [u_0(2) + u_0(1), 0]^T + \hat{\mathbf{h}}_3^\perp v_3, \quad (81)$$

where $u_0(1)$, $u_0(2)$, c_1 , c_2 and c_3 are common messages, u_j and v_j ($j=1,2,3$) are private symbols respectively intended for user 1 and 2. The power and rate allocation are given in Table II. As presented, $u_0(1)$ and $u_0(2)$ are respectively sent in subband 1 and 2 when user 1 is more capable to decode them since $a_1 > b_1$ and $a_2 > b_2$. In subband 3, $u_0(1)$ and $u_0(2)$ are transmitted again via superposition coding and user 2 has the capability to decode both of them as $q_3^- = q_1^+ + q_2^+$. The received

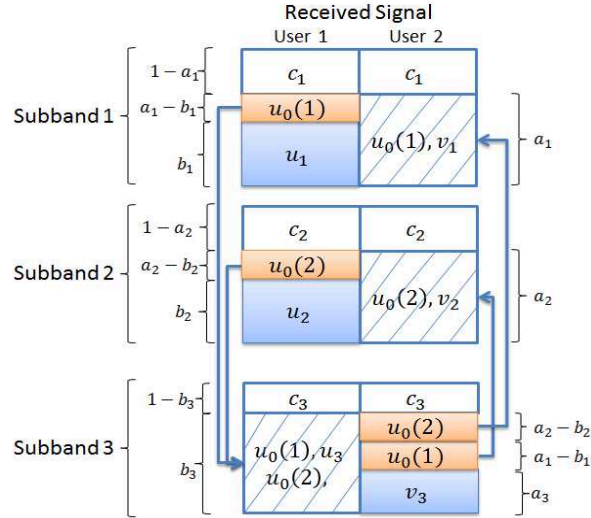


Fig. 7: The illustration of the received signal and decoding procedure of the optimal scheme for the \mathcal{P}_3 problem, where the values beside the bracket stand for the (pre-log factor of the) rate of the corresponding symbols. $u_0(1)$ and $u_0(2)$ are transmitted. User 1 decodes them in subband 1 and 2 respectively. User 2 recovers them using SIC in subband 3.

signals at user 1 and user 2 are expressed as

$$y_1 = \underbrace{h_{11}^* c_1}_P + \underbrace{\mathbf{h}_1^H \hat{\mathbf{g}}_1^\perp u_1}_{P^{b_1}} + \underbrace{h_{11}^* u_0(1)}_{P^{a_1}} + \underbrace{\mathbf{h}_1^H \hat{\mathbf{h}}_1^\perp v_1}_{P^0} + \epsilon_{11}, \quad (82)$$

$$z_1 = \underbrace{g_{11}^* c_1}_P + \underbrace{\mathbf{g}_1^H \hat{\mathbf{g}}_1^\perp u_1}_{P^0} + \underbrace{g_{11}^* u_0(1)}_{P^{a_1}} + \underbrace{\mathbf{g}_1^H \hat{\mathbf{h}}_1^\perp v_1}_{P^{a_1}} + \epsilon_{12}, \quad (83)$$

$$y_2 = \underbrace{h_{21}^* c_2}_P + \underbrace{\mathbf{h}_2^H \hat{\mathbf{g}}_2^\perp u_2}_{P^{b_2}} + \underbrace{h_{21}^* u_0(2)}_{P^{a_2}} + \underbrace{\mathbf{h}_2^H \hat{\mathbf{h}}_2^\perp v_2}_{P^0} + \epsilon_{21}, \quad (84)$$

$$z_2 = \underbrace{g_{21}^* c_2}_P + \underbrace{\mathbf{g}_2^H \hat{\mathbf{g}}_2^\perp u_2}_{P^0} + \underbrace{g_{21}^* u_0(2)}_{P^{a_2}} + \underbrace{\mathbf{g}_2^H \hat{\mathbf{h}}_2^\perp v_2}_{P^{a_2}} + \epsilon_{22}, \quad (85)$$

$$y_3 = \underbrace{h_{31}^* c_3}_P + \underbrace{\mathbf{h}_3^H \hat{\mathbf{g}}_3^\perp u_3}_{P^{b_3}} + \underbrace{h_{31}^* (u_0(2) + u_0(1))}_{P^{b_3} \quad P^{b_3 - a_2^+}} + \underbrace{\mathbf{h}_3^H \hat{\mathbf{h}}_3^\perp v_3}_{P^0} + \epsilon_{31}, \quad (86)$$

$$z_3 = \underbrace{g_{31}^* c_3}_P + \underbrace{\mathbf{g}_3^H \hat{\mathbf{g}}_3^\perp u_3}_{P^0} + \underbrace{g_{31}^* (u_0(2) + u_0(1))}_{P^{b_3} \quad P^{b_3 - a_2^+}} + \underbrace{\mathbf{g}_3^H \hat{\mathbf{h}}_3^\perp v_3}_{P^{a_3}} + \epsilon_{32}, \quad (87)$$

Decoding: At both users, the common messages c_1 , c_2 and c_3 are respectively decoded from the observation in subband 1, 2 and 3. After that, at user 1, $u_0(1)$ and $u_0(2)$ are respectively decoded from y_1 and y_2 by treating u_1 and u_2 as noise, since a_1 and a_2 are respectively greater than b_1 and b_2 . With the knowledge of $u_0(1)$ and $u_0(2)$, the private symbols u_1 , u_2 and u_3 are obtained from y_1 , y_2 and y_3 respectively using SIC.

At user 2, treating $u_0(1)$ and v_3 as noise, $u_0(2)$ is decoded from z_3 with the SNR as

$$SNR_{u_0(2)} \approx \frac{P^{b_3}}{P^{b_3 - a_2^+}} = P^{a_2^+} = P^{a_2 - b_2}, \text{ when } P \rightarrow \infty. \quad (88)$$

Removing $u_0(2)$ and treating v_3 as noise, $u_0(1)$ is decoded with the SNR as

$$SNR_{u_0(1)} \approx \frac{P^{b_3 - a_2^+}}{P^{a_3}} = P^{b_3 - a_2^+ - a_3} = P^{a_1^+} = P^{a_1 - b_1}, \text{ when } P \rightarrow \infty. \quad (89)$$

With the knowledge of $u_0(1)$ and $u_0(2)$, the private symbols v_1 , v_2 and v_3 can be decoded from z_1 , z_2 and z_3 respectively using SIC.

The private symbols u_1, u_2, u_3 intended for user 1 achieve the sum rate $(b_1 + b_2 + b_3) \log P$, so do the private symbols v_1, v_2, v_3 for user 2 since $\sum_{j=1}^3 a_j = \sum_{j=1}^3 b_j$. Considering the common messages intended for user 1 and user 2 respectively, we have the *DoF* pair $(1, \frac{1}{3} \sum_{j=1}^3 b_j)$ and $(\frac{1}{3} \sum_{j=1}^3 a_j, 1)$.

It is worth noting that for the scenario with $a_1 > b_1$, $a_2 = b_2$ and $a_3 < b_3$, the problem turns to a combination of one \mathcal{P}_1 problem (i.e. subband 2) and one \mathcal{P}_2 problem (i.e. subband 1 and 3). Specifically, the transmitted signal in subband 2 become exactly

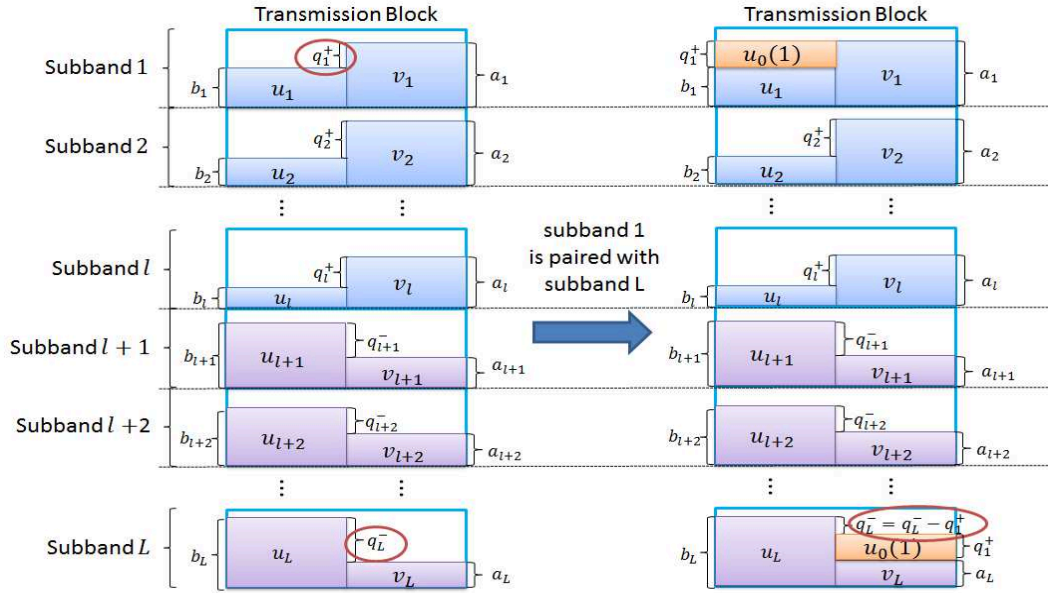


Fig. 8: The illustration of the generation of the optimal transmission block for \mathcal{P}_L problem. The values beside the brackets represent the (pre-log factor of the) rate allocated to the corresponding symbols.

the same as that in (65) because $u_0(2)$ is not generated. The transmitted signals in subband 1 and 3 follow the form as in (67) and (68) and $u_0(1)$ is the only common message II to be sent. Moreover, for the case $a_1=b_1$, $a_2=b_2$ and $a_3=b_3$, the transmitted signals in (79) to (81) degrade to (65) and no common messages II is generated.

Remark 6. [Insights behind the solution to \mathcal{P}_3]

The construction of the transmission block (shown from (79) to (81)) relates to the channel decomposition discussed in Section IV. q_1^+ and q_2^+ represent the fraction of channel use of the subchannels with PN state and q_3^- stands for that of NP state. In order to find the alternating PN/NP scenario, we recall from the further decomposition of subchannels with PN and NP states as in Section IV-B and in Figure 3. Subchannel $\hat{3}$ is further decomposed into $\hat{3}(1)$ and $\hat{3}(2)$, with channel use q_1^+ and q_2^+ respectively. Consequently, subchannels $\hat{1}$ and $\hat{3}(1)$, subchannels $\hat{2}$ and $\hat{3}(2)$ are paired. $u_0(1)$ and $u_0(2)$ are respectively the transmissions performed on those pairs of subchannels. Figure 7 illustrates the philosophy of decoding. As shown, $u_0(1)$ and $u_0(2)$ act as two separated and independent layers of the common messages. User 1 (in subband 1 and 2) and user 2 (in subband 3) are alternatively capable to decode them. Hence, the strategy in solving a \mathcal{P}_3 problem is an extension of that solving a \mathcal{P}_2 problem.

D. \mathcal{P}_L Problem

We build the optimal transmission block for the \mathcal{P}_L problem following the discussion on the \mathcal{P}_3 problem. Briefly, the private symbols in each subband is transmitted using ZFBF precoding. The rate and power allocated to them are functions of the quality of the CSIT of their unintended user. Afterwards, every common message II, namely $u_0(\cdot)$ symbol, is generated based on the insight discussed in Remark 6 and transmitted through one antenna. Finally, common message I in each subband (i.e. c_j) is transmitted through a single antenna via the remaining channel use. The procedure of generating the transmission signal is sketched below

- 1) In each subband, generate the private symbols u_j and v_j respectively with the power P^{b_j} and P^{a_j} and rate $b_j \log P$ and $a_j \log P$, $\forall j \in [1, L]$.
- 2) $i \leftarrow 1$; If $\{q^+\}$ or $\{q^-\}$ has all zero elements, goto Step 7), otherwise, goto Step 3).
- 3) Arbitrarily pair subbands $j_1 \in [1:l]$ and $j_2 \in [l+1:L]$, such that $q_{j_1}^+ \neq 0$ and $q_{j_2}^- \neq 0$.
- 4) Generate common message II, $u_0(i)$, with rate $\min(q_{j_1}^+, q_{j_2}^-) \log P$ and transmit it in subband j_1 and j_2 .
- 5) If $q_{j_1}^+ < q_{j_2}^-$, update $q_{j_2}^- \leftarrow q_{j_2}^- - q_{j_1}^+$ and $q_{j_1}^+ \leftarrow 0$; Else if $q_{j_1}^+ > q_{j_2}^-$, update $q_{j_1}^+ \leftarrow q_{j_1}^+ - q_{j_2}^-$ and $q_{j_2}^- \leftarrow 0$; Else if $q_{j_1}^+ = q_{j_2}^-$, update $q_{j_1}^+ \leftarrow 0$ and $q_{j_2}^- \leftarrow 0$.
- 6) $i \leftarrow i+1$; If $\{q^+\}$ or $\{q^-\}$ has all zero elements, goto Step 7), otherwise, goto Step 3).
- 7) For the subbands with $a_j < 1$ and $b_j < 1$, generate common message I, c_j , with rate $(1 - \max(a_j, b_j)) \log P$ and power $P - P^{\max(a_j, b_j)}$.

Figure 8 illustrates the generation of the transmission block for the \mathcal{P}_L problem. As shown, the private symbols are generated following Step 1). After that, subband 1 and subband L are paired as in Step 3), in each of which $u_0(1)$ is generated and

	Power	Rate ($\log P$)
c_j	$P - P^{a_j}$	$1 - a_j$
u_j	$P^{b_j} / 2$	b_j
v_j	$P^{a_j} / 2$	a_j
$u_0(\mathcal{K}_j(1))$	$(P^{a_j} - P^{a_j - \tau_j(1)}) / 2$	$\tau_j(1)$
$u_0(\mathcal{K}_j(2))$	$(P^{a_j - \tau_j(1)} - P^{a_j - \tau_j(1) - \tau_j(2)}) / 2$	$\tau_j(2)$
\vdots	\vdots	\vdots
$u_0(\mathcal{K}_j(K_j))$	$(P^{a_j - \sum_{i=1}^{K_j-1} \tau_j(i)} - P^{a_j - \sum_{i=1}^{K_j} \tau_j(i)}) / 2$	$\tau_j(K_j)$

 TABLE III: Power and rate allocation in the optimal scheme for \mathcal{P}_L problem in the subband with $j \in [1, l]$.

transmitted with rate $q_1^+ \log P$ following Step 4). q_1^+ becomes zero and q_3^- turns to $q_3^- - q_1^+$ according to Step 5). Keep generating $u_0(i)$ messages following Step 3) to 5) until either the set $\{q^+\}$ or $\{q^-\}$ has all zero elements.

Consequently, the transmit signal in general consists of a common message I (c_j), ZFBF-precoded private symbols (u_j and v_j) and superposition-coded multiple common messages II ($u_0(\cdot)$) symbols. It writes as

$$\mathbf{x}_j = [c_j, 0]^T + \hat{\mathbf{g}}_j^\perp u_j + \hat{\mathbf{h}}_j^\perp v_j + \left[\sum_{i=1}^{K_j=|\mathcal{K}_j|} u_0(\mathcal{K}_j(i)), 0 \right]^T, \quad (90)$$

where \mathcal{K}_j , with the cardinality K_j , is the set of the $u_0(\cdot)$ symbols to be sent in subband j . The power and rate allocation for the symbols transmitted in subband $j \in [1, l]$ are presented in Table III, where $\tau_j(i)$ represents the rate of $u_0(\mathcal{K}_j(i))$. Also, we have $P^{a_j - \sum_{i=1}^{K_j} \tau_j(i)} = P^{b_j}$, namely $\sum_{i=1}^{K_j} \tau_j(i) = a_j - b_j$, such that all the $u_0(\cdot)$ symbols in the set \mathcal{K}_j can be recovered.

The signal received at each receiver in subband $j \leq l$ is expressed as

$$y_j = \underbrace{h_{j1}^* c_j}_P + \underbrace{\mathbf{h}_j^H \hat{\mathbf{g}}_j^\perp u_j}_{P^{b_j}} + \underbrace{\mathbf{h}_j^H \hat{\mathbf{h}}_j^\perp v_j}_{P^0} + h_{j1}^* \underbrace{(u_0(\mathcal{K}_j(1)) + u_0(\mathcal{K}_j(2)) + \dots + u_0(\mathcal{K}_j(K_j)))}_{P^{a_j}} + \underbrace{\epsilon_{j1}}_{P^{a_j - \sum_{k=1}^{K_j-1} \tau_j(k)}}, \quad (91)$$

$$z_j = \underbrace{g_{j1}^* c_j}_P + \underbrace{\mathbf{g}_j^H \hat{\mathbf{g}}_j^\perp u_j}_{P^0} + \underbrace{\mathbf{g}_j^H \hat{\mathbf{h}}_j^\perp v_j}_{P^{a_j}} + g_{j1}^* \underbrace{(u_0(\mathcal{K}_j(1)) + u_0(\mathcal{K}_j(2)) + \dots + u_0(\mathcal{K}_j(K_j)))}_{P^{a_j}} + \underbrace{\epsilon_{j2}}_{P^{a_j - \sum_{k=1}^{K_j-1} \tau_j(k)}}. \quad (92)$$

Decoding: At both users, c_j can be decoded first by treating all the other terms as noise. After removing c_j , user 1 sees $u_0(\mathcal{K}_j(i)), i=1, 2, \dots, K_j$ with different power levels and decodes them using SIC. Specifically, $u_0(\mathcal{K}_j(i)), i < K_j$ is decoded with the SNR as

$$\text{SNR}_{u_0(\mathcal{K}_j(i))} \approx \frac{P^{a_j - \sum_{i'=1}^{i-1} \tau_j(i')}}{P^{a_j - \sum_{i'=1}^i \tau_j(i')}} = P^{\tau_j(i)}, \text{ when } P \rightarrow \infty. \quad (93)$$

By treating u_j as noise, $u_0(\mathcal{K}_j(K_j))$ is recovered with the SNR as

$$\text{SNR}_{u_0(\mathcal{K}_j(K_j))} \approx \frac{P^{a_j - \sum_{i'=1}^{K_j-1} \tau_j(i')}}{P^{b_j}} = P^{\tau_j(i)}, \text{ when } P \rightarrow \infty, \quad (94)$$

since $\sum_{i=1}^{K_j} \tau_j(i) = a_j - b_j$. After removing $u_0(\mathcal{K}_j(i)), i=1, 2, \dots, K_j$ from y_j , user 1 recovers u_j subject to noise.

Performing the same decoding procedure for subbands 1 to l (with $a_j \geq b_j$), user 1 can recover every $u_0(\cdot)$ symbol. However in the subbands $l+1$ to L (with $a_j \leq b_j$), user 1 sees a mixture of the $u_0(\cdot)$ message and u_j . Since every $u_0(\cdot)$ symbol is recovered from y_1 to y_l , the private symbols intended for user 1 in subbands $l+1$ to L are recovered with the knowledge of all the $u_0(\cdot)$ symbols. User 2 can decode its messages similarly.

The sum rate achieved by the private symbols, $u_{1:L}$, intended for user 1, is $\sum_{j=1}^L b_j \log P$. The private symbols, $v_{1:L}$, intended for user 2, achieve the sum rate $\sum_{j=1}^L a_j \log P$. Besides, the common messages I, $c_{1:L}$, achieve the sum rate $(L - \sum_{j=1}^L \max(a_j, b_j)) \log P$. Combined with the sum rate of common messages II ($u_0(\cdot)$), namely $\sum_{j=1}^L q_j^+ \log P = \frac{1}{2} \sum_{j=1}^L |a_j - b_j|$, the sum rate of all the symbols is $(L + \sum_{j=1}^L a_j) \log P$. If all the common messages (i.e. $u_0(\cdot)$ symbols and $c_{1:L}$) are intended for user 1, the DoF pair $(1, \frac{1}{L} \sum_{j=1}^L a_j)$ is achieved, thus solving the \mathcal{P}_L problem.

Remark 7. [Rate allocation and weights calculation]

Relating the rate of the symbols presented in Table III to the weights in (59), we find that the weighted-sum interpretation of the DoF region reveals not only the integration of FDMA, $S_3^{3/2}$ scheme and ZFBF, but also the rate allocation. To be specific, the common messages c_j are sent via FDMA. The sum rate of all common messages c_j is consistent with \tilde{r} , the fraction of channel use of the subchannels with NN state. Moreover, private symbols $u_{1:l}$ and $v_{l+1:L}$ are transmitted via ZFBF, their sum rate is equal to the weight of PP state, \bar{r} . The sum rate of all the $u_0(\cdot)$ messages reflects the fraction of channel use of subchannels with PN or NP state.

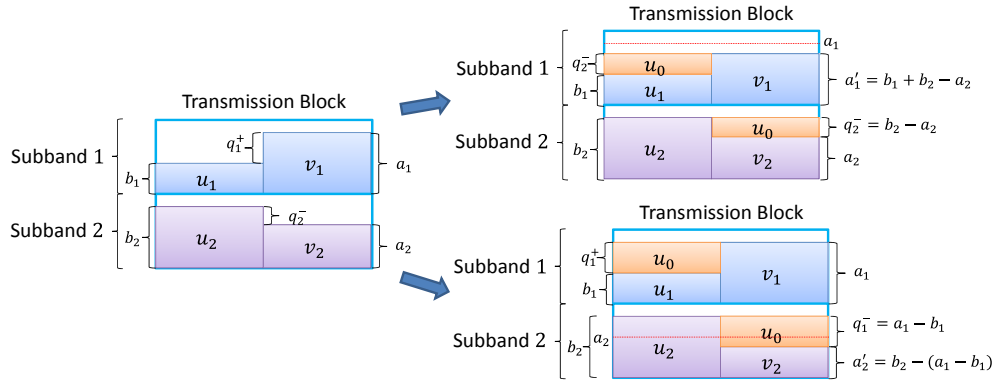


Fig. 9: The illustration of the generation of the optimal transmission block for the \mathcal{Q}_2 problem, where the values beside the bracket stand for the (pre-log factor of the) rate of the corresponding symbols. Two rate and power allocation policies are presented.

VI. ACHIEVABILITY OF \mathcal{Q}_L PROBLEM

In this section, we will focus on the category of \mathcal{Q}_L problem and work out the optimal scheme that achieves the *DoF* region specified in Theorem 1. Without loss of generality, we only investigate the \mathcal{Q}_L^+ problem as \mathcal{Q}_L^- can be solved by simply switching the role of the two users.

A. \mathcal{Q}_1^+ Problem

As a reminder, in the \mathcal{Q}_1^+ problem, we have $a_1 > b_1$. The optimal transmission strategy is straightforward and identical to that in (65) by substituting a_1 with $a_1' = b_1$. Specifically, the power and rate allocated to the private symbol v_1 is $P^{a_1'}$ and $a_1' \log P$. Since $a_1' < a_1$, v_1 is drowned by the noise in the observation of user 1. Performing the same decoding procedure as in the \mathcal{P}_1 problem, the *DoF* pair $(1, a_1') = (1, b_1)$ and $(b_1, 1)$ can be achieved.

Remark 8. [\mathcal{P}_1 and \mathcal{Q}_1]

We can conclude that the \mathcal{Q}_1^+ problem with $a_1 > b_1$ is equivalent to the \mathcal{P}_1 problem with $a_1' = b_1$ in terms of *DoF* region and the optimal transmission strategy. In other words, for a \mathcal{Q}_1^+ problem, the CSIT of user 1 is over-accurate compared to the CSIT qualities of user 2 and does not enhance the *DoF* region. We can also observe this using Corollary 1. The *DoF* region of a \mathcal{Q}_1^+ problem and a \mathcal{P}_1 problem have exactly the same weighted-sum interpretation. To be specific, after the subband in a \mathcal{Q}_1^+ problem is decomposed, the $\hat{r}' = a_1 - b_1$ channel use of the subchannel with singular PN state is merged with the subchannel with NN state. In this way, the channel use of NN state is $1 - b_1$, identical to that in a \mathcal{P}_1 problem with $a_1' = b_1$.

B. \mathcal{Q}_2^+ Problem

Similarly to the scenario considered in a \mathcal{P}_2 problem, there exists two basic scenario in a \mathcal{Q}_2^+ problem, namely 1) $a_1 \geq b_1$ and $a_2 \geq b_2$; 2) $a_1 \geq b_1$ and $a_2 < b_2$. The first case can be regarded as two \mathcal{Q}_1^+ problems or a \mathcal{Q}_1^+ problem with a \mathcal{P}_1 problem. The achievability has been studied in Section VI-A and Section V-A. For the second CSIT quality pattern, the optimal scheme is designed by reusing the philosophy of the transmission strategy discussed in Section V-B. The challenge lies in the power and rate allocation for u_0 and private symbols.

For concreteness, we initially allocate the rate of the private symbols u_j as $b_j \log P$ and v_j as $a_j \log P$. Reusing the transmission in (67) and (68), user 1 could decode u_0 with rate $q_1^+ \log P$ but user 2 could do $q_2^- \log P$. Hence, to make u_0 decodable by both users, there exist two options:

- 1) Determine the rate of u_0 as $q_2^- \log P = (b_2 - a_2) \log P$ and decrease the rate of v_1 to $a_1' \log P = (b_1 + q_2^-) \log P$ (from $a_1 \log P$);
- 2) Generate u_0 with the rate $q_1^+ \log P = (a_1 - b_1) \log P$ and reduce the rate of v_2 to $a_2' \log P = (b_2 - q_1^+) \log P$ (from $a_2 \log P$).

Figure 9 gives an illustration of these two constructions of the transmit signal. The transmitted signals write as in (67) and (68), but the power and rate allocation are changed and shown in Table IV.

Option 1	subband 1	Power	Rate (logP)	subband 2	Power	Rate (logP)
	c_1	$P - P^{q_2^- + b_1}$	$1 - q_2^- - b_1$	c_2	$P - P^{b_2}$	$1 - b_2$
u_1	$P^{b_1}/2$	b_1	u_2	$P^{b_2}/2$	b_2	
v_1	$P^{q_2^- + b_1}/2$	$q_2^- + b_1$	v_2	$P^{a_2}/2$	a_2	
u_0	$P^{q_2^- + b_1}/2 - P^{b_1}/2$	q_2^-	u_0	$P^{b_2}/2 - P^{a_2}/2$	q_2^-	
Option 2	subband 1	Power	Rate (logP)	subband 2	Power	Rate (logP)
	c_1	$P - P^{a_1}$	$1 - a_1$	c_2	$P - P^{q_1^+ + a_2}$	$1 - q_1^+ - a_2$
u_1	$P^{b_1}/2$	b_1	u_2	$P^{b_2}/2$	b_2	
v_1	$P^{a_1}/2$	a_1	v_2	$P^{b_2 - q_1^+}/2$	$b_2 - q_1^+$	
u_0	$P^{a_1}/2 - P^{b_1}/2$	q_1^+	u_0	$P^{b_2}/2 - P^{b_2 - q_1^+}/2$	q_1^+	

 TABLE IV: Power and rate allocation in the optimal scheme for the \mathcal{Q}_2 , where $q_2^- = b_2 - a_2$ and $q_1^+ = a_1 - b_1$.

Employing the first power and rate allocation policy, the signal received at each user can be written as

$$y_1 = \underbrace{h_{11}^* c_1}_P + \underbrace{\mathbf{h}_1^H \hat{\mathbf{g}}_1^\perp u_1}_{P^{b_1}} + \underbrace{h_{11}^* u_0}_{P^{q_2^- + b_1}} + \underbrace{\mathbf{h}_1^H \hat{\mathbf{h}}_1^\perp v_1}_{P^{q_2^- + b_1} P^{-a_1} < P^0} + \epsilon_{11}, \quad (95)$$

$$z_1 = \underbrace{g_{11}^* c_1}_P + \underbrace{\mathbf{g}_1^H \hat{\mathbf{g}}_1^\perp u_1}_{P^0} + \underbrace{g_{11}^* u_0}_{P^{q_2^- + b_1}} + \underbrace{\mathbf{g}_1^H \hat{\mathbf{h}}_1^\perp v_1}_{P^{q_2^- + b_1}} + \epsilon_{12}, \quad (96)$$

$$y_2 = \underbrace{h_{21}^* c_2}_P + \underbrace{\mathbf{h}_2^H \hat{\mathbf{g}}_2^\perp u_2}_{P^{b_2}} + \underbrace{h_{21}^* u_0}_{P^{b_2}} + \underbrace{\mathbf{h}_2^H \hat{\mathbf{h}}_2^\perp v_2}_{P^0} + \epsilon_{21}, \quad (97)$$

$$z_2 = \underbrace{g_{21}^* c_2}_P + \underbrace{\mathbf{g}_2^H \hat{\mathbf{g}}_2^\perp u_2}_{P^0} + \underbrace{g_{21}^* u_0}_{P^{b_2}} + \underbrace{\mathbf{g}_2^H \hat{\mathbf{h}}_2^\perp v_2}_{P^{a_2}} + \epsilon_{22}, \quad (98)$$

The decoding procedure is the same as in \mathcal{P}_2 problem discussed in Section V-B. Both users' private symbols (u_1, u_2 and v_1, v_2) achieve the sum rate $(q_2^- + b_1 + a_2) \log P = (b_1 + b_2) \log P$. Besides, the common messages c_1, c_2 and u_0 , achieving the sum rate $R_{c_1} + R_{c_2} + R_{u_0} = (2 - b_1 - b_2) \log P$, can be considered as exclusively intended for user 1 or user 2. As a consequence, the DoF pair $(1, (b_1 + b_2)/2) = (1, \min(a_e, b_e))$ and $((b_1 + b_2)/2, 1) = (\min(a_e, b_e), 1)$ are achieved.

With the second power and rate allocation policy, the received signals write as

$$y_1 = \underbrace{h_{11}^* c_1}_P + \underbrace{\mathbf{h}_1^H \hat{\mathbf{g}}_1^\perp u_1}_{P^{b_1}} + \underbrace{h_{11}^* u_0}_{P^{a_1}} + \underbrace{\mathbf{h}_1^H \hat{\mathbf{h}}_1^\perp v_1}_{P^0} + \epsilon_{11}, \quad (99)$$

$$z_1 = \underbrace{g_{11}^* c_1}_P + \underbrace{\mathbf{g}_1^H \hat{\mathbf{g}}_1^\perp u_1}_{P^0} + \underbrace{g_{11}^* u_0}_{P^{a_1}} + \underbrace{\mathbf{g}_1^H \hat{\mathbf{h}}_1^\perp v_1}_{P^{a_1}} + \epsilon_{12}, \quad (100)$$

$$y_2 = \underbrace{h_{21}^* c_2}_P + \underbrace{\mathbf{h}_2^H \hat{\mathbf{g}}_2^\perp u_2}_{P^{b_2}} + \underbrace{h_{21}^* u_0}_{P^{b_2}} + \underbrace{\mathbf{h}_2^H \hat{\mathbf{h}}_2^\perp v_2}_{P^{b_2 - q_1^+} P^{-a_2} < P^0} + \epsilon_{21}, \quad (101)$$

$$z_2 = \underbrace{g_{21}^* c_2}_P + \underbrace{\mathbf{g}_2^H \hat{\mathbf{g}}_2^\perp u_2}_{P^0} + \underbrace{g_{21}^* u_0}_{P^{b_2}} + \underbrace{\mathbf{g}_2^H \hat{\mathbf{h}}_2^\perp v_2}_{P^{b_2 - q_1^+}} + \epsilon_{22}. \quad (102)$$

Performing the same decoding procedure, the same rate pair is achieved.

Remark 9. [\mathcal{P}_2 and \mathcal{Q}_2 , extension of Remark 8]

A noteworthy observation from the above scheme is that a \mathcal{Q}_2 problem can be considered as equivalent to a \mathcal{P}_2 problem. Specifically, the first power and rate allocation strategy is identical to the optimal scheme for a \mathcal{P}_2 problem with $a'_1 = b_1 + b_2 - a_2$ while fixing b_1, b_2 and a_2 . The second allocation policy coincides with the optimal scheme for a \mathcal{P}_2 problem with $a'_2 = b_2 - (a_1 - b_1)$ while fixing b_1, b_2 and a_1 . This equivalence is due to the fact that the difference between the CSIT quality of user 1 and user 2 (i.e. $a_1 + a_2 - b_1 - b_2$), interpreted as the singular \hat{r}' PN state according to the discussion in Section IV, does not benefit the DoF region more than a NN state based on Theorem 1.

C. \mathcal{Q}_L^+ Problem

Following Remark 8 and 9, to design the optimal scheme for the \mathcal{Q}_L^+ problem, we establish a \mathcal{P}_L problem with $\{a'_1, a'_2, \dots, a'_L\}$ and $\{b_1, b_2, \dots, b_L\}$, such that

$$\sum_{j=1}^L a'_j = \sum_{j=1}^L b_j, \quad (103)$$

$$a'_j \leq a_j, \forall j \in [1, L]. \quad (104)$$

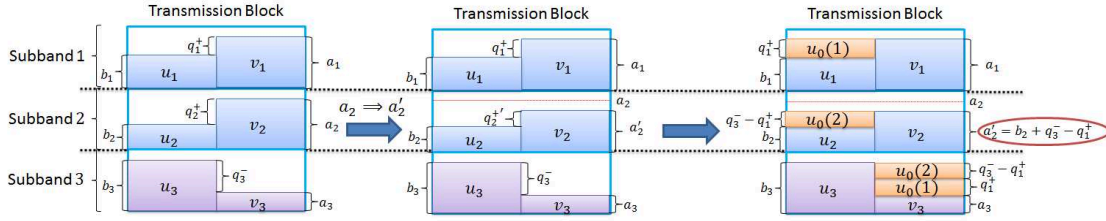


Fig. 10: The illustration of the generation of the transmission block of the optimal scheme for the \mathcal{Q}_3 problem, where the values beside the bracket stand for the (pre-log factor of the) rate of the corresponding symbols. The \mathcal{Q}_3 problem is transformed to a \mathcal{P}_3 problem and solved.

After that, the optimal transmission block for the \mathcal{Q}_L^+ problem is constructed following the footsteps presented in Section V-D. Here we do not rewrite the transmitted and received signals as they are similar to that in Section V-D. Instead, we only explain how the corner points, $(1, b_e)$ and $(b_e, 1)$, are achieved.

According to Step 1) in the procedure given in Section V-D, the power allocated to v_j (the private symbol intended for user 2 in subband j) scales as $P^{a'_j}$. This does not introduce interference to the received signal at user 1 since $\mathbf{h}_j^H \hat{\mathbf{h}}_j^\perp \sim P^{-a_j}$ and $a'_j \leq a_j$. Therefore, the sum rate of $u_{1:L}$ and $v_{1:L}$ respectively become $\sum_{j=1}^L b_j \log P$ and $\sum_{j=1}^L a'_j \log P$. The common messages II, $u_0(\cdot)$, are generated following Step 3) to 6). The sum rate of $u_0(\cdot)$ is $(\sum_{a'_j > b_j} a'_j - b_j) \log P$ because all the common messages are transmitted twice, i.e. once in the subbands with $a'_j > b_j$ and once in the subbands with $b_j > a'_j$. According to Step 7), common messages I, $c_{1:L}$ achieve the rate of $(L - \sum_{j=1}^L \max(a'_j, b_j)) \log P$. Considering all the common messages I and II are intended for user 1, we have d_1 computed as

$$d_1 = \frac{1}{L} \left(\sum_{j=1}^L b_j + \sum_{a'_j > b_j} a'_j - b_j + L - \sum_{j=1}^L \max(a'_j, b_j) \right) \quad (105)$$

$$= \frac{1}{L} \left(\sum_{j=1}^L b_j + \sum_{a'_j \geq b_j} a'_j - b_j + L - \sum_{a'_j \geq b_j} a'_j - \sum_{a'_j < b_j} b_j \right) \quad (106)$$

$$= \frac{1}{L} \left(\sum_{a'_j \geq b_j} b_j + \sum_{a'_j < b_j} b_j + \sum_{a'_j \geq b_j} a'_j - \sum_{a'_j \geq b_j} b_j + L - \sum_{a'_j \geq b_j} a'_j - \sum_{a'_j < b_j} b_j \right) \quad (107)$$

$$= 1. \quad (108)$$

(107) follows the fact that $\sum_{j=1}^L b_j = \sum_{a'_j \geq b_j} b_j + \sum_{a'_j < b_j} b_j$. Hence, the *DoF* pair $(d_1, d_2) = (1, \frac{1}{L} \sum_{j=1}^L a'_j) = (1, b_e)$ is achieved. Similarly, assuming the common messages I and II are intended for user 2, the *DoF* pair $(b_e, 1)$ is achieved.

For concreteness, we consider a \mathcal{Q}_3^+ problem with $a_1 > b_1$, $a_2 > b_2$ and $a_3 < b_3$, namely $q_1^+ + q_2^+ > q_3^-$. As shown in Figure 10, the construction of the transmission block is obtained by establishing a \mathcal{P}_3 problem with $a'_1 = a_1$, $a'_2 = b_1 + b_2 + b_3 - a_1 - a_3$ and $a'_3 = a_3$. Besides, we assume $a'_2 > 0$ and $a'_2 > b_2$. The transmitted signals write as

$$\mathbf{x}_1 = \underbrace{[c_1, 0]^T}_{P - P^{a_1}} + \underbrace{\hat{\mathbf{g}}_1^\perp u_1}_{P^{b_1/2}} + \underbrace{[u_0(1), 0]^T}_{(P^{a_1} - P^{b_1})/2} + \underbrace{\hat{\mathbf{h}}_1^\perp v_1}_{P^{a_1/2}} \quad (109)$$

$$\mathbf{x}_2 = \underbrace{[c_2, 0]^T}_{P - P^{a'_2}} + \underbrace{\hat{\mathbf{g}}_2^\perp u_2}_{P^{b_2/2}} + \underbrace{[u_0(2), 0]^T}_{(P^{a'_2} - P^{b_2})/2} + \underbrace{\hat{\mathbf{h}}_2^\perp v_2}_{P^{a'_2/2}} \quad (110)$$

$$\mathbf{x}_3 = \underbrace{[c_3, 0]^T}_{P - P^{b_3}} + \underbrace{\hat{\mathbf{g}}_3^\perp u_3}_{P^{b_3/2}} + \underbrace{[u_0(2), 0]^T}_{(P^{b_3} - P^{b_3 - q_3^- + q_1^+})/2} + \underbrace{[u_0(1), 0]^T}_{(P^{b_3 - q_3^- + q_1^+} - P^{a_3})/2} + \underbrace{\hat{\mathbf{h}}_3^\perp v_3}_{P^{a_3/2}} \quad (111)$$

The received signal can be derived similarly as that in (82) to (87). The decoding procedure follows as that in \mathcal{P}_3 problem (see Figure 7). Generally, both user recover c_1 , c_2 and c_3 from their observations by treating all the other terms as noise. Then user 1 can decode the $u_0(1)$ and $u_0(2)$ from y_1 and y_2 (the subbands with $a_j > b_j$) respectively while user 2 recovers them from z_3 (the subbands with $a_j < b_j$). With the knowledge of $u_0(1)$ and $u_0(2)$, all the private messages are decoded.

The private symbols u_1, u_2, u_3 achieve the sum rate $(b_1 + b_2 + b_3) \log P$ while the private symbols v_1, v_2, v_3 achieve the sum-rate $(a_1 + a'_2 + a_3) \log P$. Considering that c_1 , c_2 , c_3 , $u_0(1)$ and $u_0(2)$ are intended for user 1 and user 2, the *DoF* pair $(1, \frac{1}{3}(b_1 + b_2 + b_3))$ and $(\frac{1}{3}(a_1 + a'_2 + a_3), 1)$ are respectively obtained.

Remark 10. [Transmission Strategies vs. Feedback Quality Distribution]

For an L -subband scenario with given a_e and b_e , the optimal transmission strategy proposed in Section V-D and VI-C provide a general solution to achieve the optimal DoF region. However, the form of the transmitted signal in each subband varies depending on the CSIT quality pattern.

For instance, with CSIT quality pattern $a_j \geq b_j, \forall j \in [1:L]$, the L -subband scenario comprises L times of \mathcal{P}_1 or \mathcal{Q}_1 problems. The transmitted signal in each subband is independent to each other and no common messages II, namely $u_0(\cdot)$, is generated. Moreover, with per-user average CSIT quality $a_e = b_e$, an extreme scenario is defined as $(a_j, b_j) = (1, 1), \forall j \in [1, a_e \times L]$ and $(a_j, b_j) = (0, 0), \forall j \in [a_e \times L + 1, L]$, which means that the CSIT states are PP for subbands 1 to $a_e L$ while they are NN for the remaining subbands. Hence, the optimal schemes become ZFBF in subband 1 to $a_e L$ while the optimal schemes in the remaining subbands degrade to FDMA.

For a \mathcal{P}_L problem with the CSIT quality pattern satisfying the condition that $\forall \mathcal{J} \subset [1:L], \sum_{j \in \mathcal{J}} a_j \neq \sum_{j \in \mathcal{J}} b_j$, there are totally $L-1$ $u_0(\cdot)$ symbols generated and the transmitted signal in each subband is correlated to each other. Besides, there are multiple stages in the SIC and the decoding of private symbols rely on the $u_0(\cdot)$ symbols.

VII. CONCLUSION

In this contribution, we investigate a general two-user frequency correlated MISO BC, which consists of multiple subbands with varying CSIT qualities. A tight outer-bound to the DoF region is found with the help of Nair-Gamal's bound [26], Extremal Inequality [27] and Lemma 1 in [3]. Its optimality is shown by a transmission block as an extension of the optimal scheme for a two-subband scenario. Due to the varying CSIT qualities, the two users are alternatively capable of decoding the common messages $u_0(\cdot)$. To achieve the optimal DoF performance, the number of the common messages $u_0(\cdot)$ and the rate of each $u_0(\cdot)$ message are determined accordingly. It is worth noting that the optimal DoF region is a function of the minimum average CSIT quality between the two users. This result provides confirmative answer to the conjecture made in [2] that the DoF region in the two-user MISO BC with perfect CSIT of only one user is the same as that with no CSIT of either user.

This optimal DoF region is interpreted as the weighted-sum of the optimal DoF region in the CSIT states PP, PN/NP and NN. The weight of each CSIT state is calculated according to the CSIT qualities of both users in each subband and indicates the fraction of channel use of each type of CSIT states. For a fixed per-user average CSIT, the distribution of the CSIT qualities of each user across the L subbands only impacts the formation of the optimal DoF region, but does not influence the shape of the region. This sheds light on the construction of the optimal transmission scheme.

APPENDIX-DERIVATION OF (27)

To obtain (27), we introduce

$$\Phi_j = \Phi_j^{(1)} + \Phi_j^{(2)}, \text{ for } j=1, 2, \dots, \lfloor \frac{n+1}{2} \rfloor, \quad (112)$$

$$\Theta_j = \Theta_j^{(1)} + \Theta_j^{(2)}, \text{ for } j=1, 2, \dots, n, \quad (113)$$

where

$$\Phi_j^{(1)} = I(M_1, Z_{n-j+2}^n; Y_j^{n-j+1} | \mathcal{S}_1^n, Y_1^{j-1}), \quad (114)$$

$$\Phi_j^{(2)} = I(M_2; Z_j^{n-j+1} | M_1, \mathcal{S}_1^n, Y_1^{j-1}, Z_{n-j+2}^n), \quad (115)$$

$$\Theta_j^{(1)} = I(M_1, Y_1^{j-1}, Z_{j+1}^n, \hat{\mathcal{S}}_1^n; Y_j | \mathcal{S}_1^n), \quad (116)$$

$$\Theta_j^{(2)} = I(M_2, Y_1^{j-1}, Z_{j+1}^n, \hat{\mathcal{S}}_1^n; Z_j | M_1, \mathcal{S}_1^n, Y_1^{j-1}, Z_{j+1}^n). \quad (117)$$

Consequently, (27) can be rewritten as

$$\Phi_1 \leq \sum_{j=1}^n \Theta_j. \quad (118)$$

In order to show that (118) holds, we need the following upper-bounds of $\Phi_j, \forall j \leq \lfloor \frac{n+1}{2} \rfloor$, namely

$$\Phi_{j < \lfloor \frac{n+1}{2} \rfloor} \leq \Theta_j + \Theta_{n-j+1} + \Phi_{j+1}, \quad (119)$$

$$\Phi_{\lfloor \frac{n+1}{2} \rfloor} \leq \begin{cases} \Theta_{\lfloor \frac{n+1}{2} \rfloor} + \Theta_{\lfloor \frac{n+1}{2} \rfloor + 1}, & \text{if } n \text{ is even;} \\ \Theta_{\lfloor \frac{n+1}{2} \rfloor}, & \text{if } n \text{ is odd.} \end{cases} \quad (120)$$

Using (119) and (120), the summation of $\Phi_j, \forall j \leq \lfloor \frac{n+1}{2} \rfloor$ is bounded as

$$\sum_{j=1}^{\lfloor \frac{n+1}{2} \rfloor - 1} \Phi_j + \Phi_{\lfloor \frac{n+1}{2} \rfloor} \leq \sum_{j=1}^{\lfloor \frac{n+1}{2} \rfloor - 1} \{\Theta_j + \Theta_{n-j+1} + \Phi_{j+1}\} + \begin{cases} \Theta_{\lfloor \frac{n+1}{2} \rfloor} + \Theta_{\lfloor \frac{n+1}{2} \rfloor + 1}, & \text{if } n \text{ is even;} \\ \Theta_{\lfloor \frac{n+1}{2} \rfloor}, & \text{if } n \text{ is odd} \end{cases} \quad (121)$$

$$= \sum_{j=2}^{\lfloor \frac{n+1}{2} \rfloor} \Phi_j + \underbrace{\sum_{j=1}^{\lfloor \frac{n+1}{2} \rfloor - 1} \{\Theta_j + \Theta_{n-j+1}\}}_{\sum_{j=1}^n \Theta_j} + \begin{cases} \Theta_{\lfloor \frac{n+1}{2} \rfloor} + \Theta_{\lfloor \frac{n+1}{2} \rfloor + 1}, & \text{if } n \text{ is even;} \\ \Theta_{\lfloor \frac{n+1}{2} \rfloor}, & \text{if } n \text{ is odd} \end{cases} \quad (122)$$

Eliminating $\Phi_2, \Phi_3, \dots, \Phi_{\lfloor \frac{n+1}{2} \rfloor}$ in both l.h.s and r.h.s, (118) holds. Next, we aim at showing (119) and (120).

A. When $j < \lfloor \frac{n+1}{2} \rfloor$

$\Phi_j^{(1)}$ is derived as follows.

$$\Phi_j^{(1)} = I(M_1, Z_{n-j+2}^n; Y_{n-j+1} | \mathcal{S}_1^n, Y_1^{n-j}) + I(M_1, Z_{n-j+2}^n; Y_j^{n-j} | \mathcal{S}_1^n, Y_1^{j-1}) \quad (123)$$

$$\leq I(M_1, Z_{n-j+2}^n, Y_1^{n-j}; Y_{n-j+1} | \mathcal{S}_1^n) + I(M_1, Z_{n-j+2}^n; Y_j | \mathcal{S}_1^n, Y_1^{j-1}) + I(M_1, Z_{n-j+2}^n; Y_{j+1}^{n-j} | \mathcal{S}_1^n, Y_1^j) \quad (124)$$

$$= I(M_1, Z_{n-j+2}^n, Y_1^{n-j}; Y_{n-j+1} | \mathcal{S}_1^n) + I(M_1, Z_{n-j+2}^n, Y_1^{j-1}; Y_j | \mathcal{S}_1^n, M_1, Z_{n-j+2}^n, Y_1^{j-1}) + I(M_1, Z_{n-j+2}^n, Y_1^j; Y_{j+1}^{n-j} | \mathcal{S}_1^n, M_1, Z_{n-j+2}^n, Y_1^j) \quad (125)$$

$$\leq \underbrace{I(M_1, Z_{n-j+2}^n, Y_1^{n-j}, \hat{\mathcal{S}}_1^n; Y_{n-j+1} | \mathcal{S}_1^n)}_{\Theta_{n-j+1}^{(1)}} + \underbrace{I(M_1, Z_{n-j+2}^n, Y_1^{j-1}, \hat{\mathcal{S}}_1^n; Y_j | \mathcal{S}_1^n)}_{\Theta_j^{(1)}} + I(M_1, Z_{n-j+2}^n, Y_1^j; Y_{j+1}^{n-j} | \mathcal{S}_1^n, Y_1^j)$$

$$= \underbrace{I(M_1, Z_{n-j+2}^n; Y_{j+1}^{n-j} | \mathcal{S}_1^n, Y_1^j)}_{\Phi_{j+1}^{(1)}} - I(Z_{n-j+2}^{n-j+1}; Y_j | \mathcal{S}_1^n, M_1, Z_{n-j+2}^n, Y_1^{j-1}) - I(Z_{n-j+2}^{n-j+1}; Y_{j+1}^{n-j} | \mathcal{S}_1^n, M_1, Z_{n-j+2}^n, Y_1^j) \quad (126)$$

$$= \Theta_j^{(1)} + \Theta_{n-j+1}^{(1)} + \Phi_{j+1}^{(1)} - I(Z_{n-j+2}^{n-j+1}; Y_j | \mathcal{S}_1^n, M_1, Z_{n-j+2}^n, Y_1^{j-1}) - I(Z_{n-j+2}^{n-j+1}; Y_{j+1}^{n-j} | \mathcal{S}_1^n, M_1, Z_{n-j+2}^n, Y_1^j). \quad (127)$$

The derivations follow the chain rule of mutual information. The inequality in (124) and (126) are due to the fact that removing the condition does not reduce the mutual information (e.g. $I(A; B|C) = I(A, C; B|C) \leq I(A, C; B)$).

When $j < \lfloor \frac{n+1}{2} \rfloor$, $\Phi_j^{(2)}$ is derived as

$$\Phi_j^{(2)} = I(M_2; Z_j | M_1, \mathcal{S}_1^n, Y_1^{j-1}, Z_{j+1}^n) + I(M_2; Z_{n-j+1}^{n-j+1} | \mathcal{S}_1^n, M_1, Y_1^{j-1}, Z_{n-j+2}^n) \quad (128)$$

$$= I(M_2, \hat{\mathcal{S}}_1^n, Y_1^{j-1}, Z_{j+1}^n; Z_j | M_1, \mathcal{S}_1^n, Y_1^{j-1}, Z_{j+1}^n) + I(M_2; Z_{n-j+1} | \mathcal{S}_1^n, M_1, Y_1^{j-1}, Z_{n-j+2}^n) + I(M_2; Z_{n-j+1}^{n-j} | \mathcal{S}_1^n, M_1, Y_1^{j-1}, Z_{n-j+1}^n) \quad (129)$$

$$\leq I(M_2, \hat{\mathcal{S}}_1^n, Y_1^{j-1}, Z_{j+1}^n; Z_j | M_1, \mathcal{S}_1^n, Y_1^{j-1}, Z_{j+1}^n) + I(M_2, Y_j^{n-j}; Z_{n-j+1} | \mathcal{S}_1^n, M_1, Y_1^{j-1}, Z_{n-j+2}^n) + I(M_2, Y_j; Z_{n-j+1}^{n-j} | \mathcal{S}_1^n, M_1, Y_1^{j-1}, Z_{n-j+1}^n) \quad (130)$$

$$= I(M_2, \hat{\mathcal{S}}_1^n, Y_1^{j-1}, Z_{j+1}^n; Z_j | M_1, \mathcal{S}_1^n, Y_1^{j-1}, Z_{j+1}^n) + I(M_2; Z_{n-j+1} | \mathcal{S}_1^n, M_1, Y_1^{n-j}, Z_{n-j+2}^n) + I(Y_j^{n-j}; Z_{n-j+1} | \mathcal{S}_1^n, M_1, Y_1^{j-1}, Z_{n-j+2}^n) + I(M_2; Z_{n-j+1}^{n-j} | \mathcal{S}_1^n, M_1, Y_1^j, Z_{n-j+1}^n) + I(Y_j; Z_{n-j+1}^{n-j} | \mathcal{S}_1^n, M_1, Y_1^{j-1}, Z_{n-j+1}^n) \quad (131)$$

$$= \underbrace{I(M_2, \hat{\mathcal{S}}_1^n, Y_1^{j-1}, Z_{j+1}^n; Z_j | M_1, \mathcal{S}_1^n, Y_1^{j-1}, Z_{j+1}^n)}_{\Theta_j^{(2)}} + \underbrace{I(M_2, Y_1^{n-j}, Z_{n-j+2}^n, \hat{\mathcal{S}}_1^n; Z_{n-j+1} | \mathcal{S}_1^n, M_1, Y_1^{n-j}, Z_{n-j+2}^n)}_{\Theta_{n-j+1}^{(2)}} + I(M_2; Z_{n-j+1}^{n-j} | \mathcal{S}_1^n, M_1, Y_1^j, Z_{n-j+1}^n)$$

$$= \underbrace{I(M_2; Z_{n-j+1}^{n-j} | \mathcal{S}_1^n, M_1, Y_1^j, Z_{n-j+1}^n)}_{\Phi_{j+1}^{(2)}} + I(Y_j^{n-j}; Z_{n-j+1} | \mathcal{S}_1^n, M_1, Y_1^{j-1}, Z_{n-j+2}^n) + I(Y_j; Z_{n-j+1}^{n-j} | \mathcal{S}_1^n, M_1, Y_1^{j-1}, Z_{n-j+1}^n) \quad (132)$$

$$= \Theta_j^{(2)} + \Theta_{n-j+1}^{(2)} + \Phi_{j+1}^{(2)} + I(Y_j^{n-j}; Z_{n-j+1} | \mathcal{S}_1^n, M_1, Y_1^{j-1}, Z_{n-j+2}^n) + I(Y_j; Z_{n-j+1}^{n-j} | \mathcal{S}_1^n, M_1, Y_1^{j-1}, Z_{n-j+1}^n). \quad (133)$$

The derivations follow the chain rule of mutual information. (130) results from adding Y_j^{n-j} and Y_j respectively in the last two terms increases the mutual information (e.g. $I(A; B|C) \leq I(A, D; B|C)$, the equality holds if and only if D is deterministic function of C).

Combining (127) and (133) yields

$$\Phi_j = \Phi_j^{(1)} + \Phi_j^{(2)} \quad (134)$$

$$\begin{aligned} &\leq \Theta_j^{(1)} + \Theta_{n-j+1}^{(1)} + \Phi_{j+1}^{(1)} + \Theta_j^{(2)} + \Theta_{n-j+1}^{(2)} + \Phi_{j+1}^{(2)} \\ &\quad + I(Y_j^{n-j}; Z_{n-j+1} | \mathcal{S}_1^n, M_1, Y_1^{j-1}, Z_{n-j+2}^n) + I(Y_j; Z_{j+1}^{n-j} | \mathcal{S}_1^n, M_1, Y_1^{j-1}, Z_{n-j+1}^n) \\ &\quad - I(Z_{j+1}^{n-j+1}; Y_j | \mathcal{S}_1^n, M_1, Z_{n-j+2}^n, Y_1^{j-1}) - I(Z_{n-j+1}; Y_{j+1}^{n-j} | \mathcal{S}_1^n, M_1, Z_{n-j+2}^n, Y_1^j) \end{aligned} \quad (135)$$

$$\begin{aligned} &= \Theta_j + \Theta_{n-j+1} + \Phi_{j+1} \\ &\quad + I(Y_j; Z_{n-j+1} | \mathcal{S}_1^n, M_1, Y_1^{j-1}, Z_{n-j+2}^n) + I(Y_{j+1}^{n-j}; Z_{n-j+1} | \mathcal{S}_1^n, M_1, Y_1^j, Z_{n-j+2}^n) \\ &\quad + I(Y_j; Z_{j+1}^{n-j} | \mathcal{S}_1^n, M_1, Y_1^{j-1}, Z_{n-j+1}^n) \\ &\quad - I(Z_{n-j+1}; Y_j | \mathcal{S}_1^n, M_1, Z_{n-j+2}^n, Y_1^{j-1}) - I(Z_{j+1}^{n-j}; Y_j | \mathcal{S}_1^n, M_1, Z_{n-j+1}^n, Y_1^{j-1}) \\ &\quad - I(Z_{n-j+1}; Y_{j+1}^{n-j} | \mathcal{S}_1^n, M_1, Z_{n-j+2}^n, Y_1^j) \end{aligned} \quad (136)$$

$$= \Theta_j + \Theta_{n-j+1} + \Phi_{j+1}. \quad (137)$$

B. When $j = \lfloor \frac{n+1}{2} \rfloor$

1) n is an even number: In this case, $j = \lfloor \frac{n+1}{2} \rfloor = \frac{n}{2}$. Following (123), (125) and (126), we have

$$\Phi_{\frac{n}{2}}^{(1)} = I(M_1, Z_{\frac{n}{2}+2}^n; Y_{\frac{n}{2}+1} | \mathcal{S}_1^n, Y_1^{\frac{n}{2}}) + I(M_1, Z_{\frac{n}{2}+2}^n; Y_{\frac{n}{2}} | \mathcal{S}_1^n, Y_1^{\frac{n}{2}-1}) \quad (138)$$

$$\leq I(M_1, Z_{\frac{n}{2}+2}^n, Y_1^{\frac{n}{2}}; Y_{\frac{n}{2}+1} | \mathcal{S}_1^n) + I(M_1, Z_{\frac{n}{2}+2}^n; Y_{\frac{n}{2}} | \mathcal{S}_1^n, Y_1^{\frac{n}{2}-1}) \quad (139)$$

$$\begin{aligned} &= I(M_1, Z_{\frac{n}{2}+2}^n, Y_1^{\frac{n}{2}}; Y_{\frac{n}{2}+1} | \mathcal{S}_1^n) + I(M_1, Z_{\frac{n}{2}+1}^n; Y_{\frac{n}{2}} | \mathcal{S}_1^n, Y_1^{\frac{n}{2}-1}) \\ &\quad - I(Z_{\frac{n}{2}+1}; Y_{\frac{n}{2}} | \mathcal{S}_1^n, M_1, Z_{\frac{n}{2}+2}^n, Y_1^{\frac{n}{2}-1}) \end{aligned} \quad (140)$$

$$\begin{aligned} &\leq \underbrace{I(M_1, Z_{\frac{n}{2}+2}^n, Y_1^{\frac{n}{2}}, \hat{\mathcal{S}}_1^n; Y_{\frac{n}{2}+1} | \mathcal{S}_1^n)}_{\Theta_{\frac{n}{2}+1}} + \underbrace{I(M_1, Z_{\frac{n}{2}+1}^n, Y_1^{\frac{n}{2}-1}, \hat{\mathcal{S}}_1^n; Y_{\frac{n}{2}} | \mathcal{S}_1^n)}_{\Theta_{\frac{n}{2}}} \\ &\quad - I(Z_{\frac{n}{2}+1}; Y_{\frac{n}{2}} | \mathcal{S}_1^n, M_1, Z_{\frac{n}{2}+2}^n, Y_1^{\frac{n}{2}-1}). \end{aligned} \quad (141)$$

$\Phi_{\frac{n}{2}}^{(2)}$ is derived similar as (128)-(132), namely

$$\Phi_{\frac{n}{2}}^{(2)} = I(M_2; Z_{\frac{n}{2}} | M_1, \mathcal{S}_1^n, Y_1^{\frac{n}{2}-1}, Z_{\frac{n}{2}+1}^n) + I(M_2; Z_{\frac{n}{2}+1} | \mathcal{S}_1^n, M_1, Y_1^{\frac{n}{2}-1}, Z_{\frac{n}{2}+2}^n) \quad (142)$$

$$= \underbrace{I(M_2, \hat{\mathcal{S}}_1^n, Y_1^{\frac{n}{2}-1}, Z_{\frac{n}{2}+1}^n; Z_{\frac{n}{2}} | M_1, \mathcal{S}_1^n, Y_1^{\frac{n}{2}-1}, Z_{\frac{n}{2}+1}^n)}_{\Theta_{\frac{n}{2}}} + I(M_2; Z_{\frac{n}{2}+1} | \mathcal{S}_1^n, M_1, Y_1^{\frac{n}{2}-1}, Z_{\frac{n}{2}+2}^n) \quad (143)$$

$$\leq \Theta_{\frac{n}{2}} + I(M_2, Y_{\frac{n}{2}}; Z_{\frac{n}{2}+1} | \mathcal{S}_1^n, M_1, Y_1^{\frac{n}{2}-1}, Z_{\frac{n}{2}+2}^n) \quad (144)$$

$$= \Theta_{\frac{n}{2}} + I(M_2; Z_{\frac{n}{2}+1} | \mathcal{S}_1^n, M_1, Y_1^{\frac{n}{2}}, Z_{\frac{n}{2}+2}^n) + I(Y_{\frac{n}{2}}; Z_{\frac{n}{2}+1} | \mathcal{S}_1^n, M_1, Y_1^{\frac{n}{2}-1}, Z_{\frac{n}{2}+2}^n) \quad (145)$$

$$= \Theta_{\frac{n}{2}} + \underbrace{I(M_2, \hat{\mathcal{S}}_1^n, Y_1^{\frac{n}{2}}, Z_{\frac{n}{2}+2}^n; Z_{\frac{n}{2}+1} | \mathcal{S}_1^n, M_1, Y_1^{\frac{n}{2}}, Z_{\frac{n}{2}+2}^n)}_{\Theta_{\frac{n}{2}+1}} + I(Y_{\frac{n}{2}}; Z_{\frac{n}{2}+1} | \mathcal{S}_1^n, M_1, Y_1^{\frac{n}{2}-1}, Z_{\frac{n}{2}+2}^n) \quad (146)$$

Adding (141) and (146), (120) holds.

2) n is an odd number: In this case, $\lfloor \frac{n+1}{2} \rfloor = \frac{n+1}{2}$. We can rewrite $\Phi_{\frac{n+1}{2}}^{(1)}$ and $\Phi_{\frac{n+1}{2}}^{(2)}$ as

$$\Phi_{\frac{n+1}{2}}^{(1)} = I(M_1, Z_{\frac{n+1}{2}+1}^n; Y_{\frac{n+1}{2}}^n | \mathcal{S}_1^n, Y_1^{\frac{n+1}{2}-1}) \quad (147)$$

$$= I(M_1, Z_{\frac{n+1}{2}+1}^n, Y_1^{\frac{n+1}{2}-1}, \hat{\mathcal{S}}_1^n; Y_{\frac{n+1}{2}}^n | \mathcal{S}_1^n, Y_1^{\frac{n+1}{2}-1}), \quad (148)$$

$$\Phi_{\frac{n+1}{2}}^{(2)} = I(M_2; Z_{\frac{n+1}{2}}^n | M_1, \mathcal{S}_1^n, Y_1^{\frac{n+1}{2}-1}, Z_{\frac{n+1}{2}+1}^n) \quad (149)$$

$$= I(M_2, Y_1^{\frac{n+1}{2}-1}, Z_{\frac{n+1}{2}+1}^n, \hat{\mathcal{S}}_1^n; Z_{\frac{n+1}{2}}^n | M_1, \mathcal{S}_1^n, Y_1^{\frac{n+1}{2}-1}, Z_{\frac{n+1}{2}+1}^n). \quad (150)$$

Consequently, (120) holds after adding (148) and (150).

REFERENCES

- [1] M. Maddah-Ali and D. Tse, "Completely stale transmitter channel state information is still very useful," *IEEE Trans. Inf. Theory*, vol. 58, no. 7, pp. 4418–4431, July 2012.
- [2] R. Tandon, S. Jafar, S. Shamai Shitz, and H. Poor, "On the synergistic benefits of alternating csit for the miso broadcast channel," *IEEE Trans. Inf. Theory*, vol. 59, pp. 4106–4128, July 2013.
- [3] S. Yang, M. Kobayashi, D. Gesbert, and X. Yi, "Degrees of freedom of time correlated miso broadcast channel with delayed csit," *IEEE Trans. Inf. Theory*, vol. 59, pp. 315–328, Jan. 2013.
- [4] M. Kobayashi, S. Yang, D. Gesbert, and X. Yi, "On the degrees of freedom of time correlated miso broadcast channel with delayed csit," in *Information Theory Proceedings (ISIT), 2012 IEEE International Symposium on*, Cambridge, MA, USA, 2012, pp. 2501–2505.
- [5] T. Gou and S. Jafar, "Optimal use of current and outdated channel state information: Degrees of freedom of the miso bc with mixed csit," *IEEE Comms. Letters*, vol. 16, no. 7, pp. 1084–1087, July 2012.
- [6] J. Chen and P. Elia, "Degrees-of-freedom region of the miso broadcast channel with general mixed-csit," vol. arxiv/1205.3474, May, 2012.
- [7] C. Hao and B. Clerckx, "Degrees-of-freedom region of time correlated miso broadcast channel with perfect delayed csit and asymmetric partial current csit," available on arXiv: 1211.4381, 2012.
- [8] J. Chen and P. Elia, "Can imperfect delayed csit be as useful as perfect delayed csit? dof analysis and constructions for the bc," in *Communication, Control, and Computing (Allerton), 2012 50th Annual Allerton Conference on*, Monticello, IL, 2012, pp. 1254–1261.
- [9] —, "Toward the performance vs. feedback tradeoff for the two-user miso broadcast channel," submitted to *IEEE Trans. Inf. Theory*, November 2012, vol. available on arXiv:1306.1751., 2013.
- [10] X. Yi, S. Yang, D. Gesbert, and M. Kobayashi, "The degrees of freedom region of temporally-correlated mimo networks with delayed csit," submitted to *IEEE Trans. on Info. Theory*, vol. arXiv preprint arXiv: 1211.3322., Oct. 2012.
- [11] X. Yi, D. Gesbert, S. Yang, and M. Kobayashi, "Degrees of freedom of time-correlated broadcast channels with delayed CSIT: The MIMO case," in *ISIT 2013, IEEE International Symposium on Information Theory, July 7-12, 2013, Istanbul, TURKEY*, July 2013. [Online]. Available: <http://www.eurecom.fr/publication/4023>
- [12] J. Chen and P. Elia, "Symmetric two-user mimo bc and ic with evolving feedback," available on arXiv:1306.3710, 2013.
- [13] C. Vaze and M. Varanasi, "The degree-of-freedom regions of mimo broadcast, interference, and cognitive radio channels with no csit," *IEEE Trans. Inf. Theory*, vol. 58, no. 8, pp. 5354–5374, Aug. 2012.
- [14] —, "The degrees of freedom region of the two-user mimo broadcast channel with delayed csit," in *Proc. IEEE Int. Symp. Inf. Theory (ISIT)*, Aug. 2011, pp. 199–203.
- [15] C. Huang, S. Jafar, S. Shamai, and S. Vishwanath, "On degrees of freedom region of mimo networks without channel state information at transmitters," *IEEE Trans. Inf. Theory*, vol. 58, no. 2, pp. 849–857, Feb. 2012.
- [16] N. Lee and R. Heath, "Not too delayed csit achieves the optimal degrees of freedom," in *Communication, Control, and Computing (Allerton), 2012 50th Annual Allerton Conference on*, Monticello, IL, 2012, pp. 1262–1269.
- [17] R. Tandon, S. A. Jafar, and S. Shamai, "Minimum csit to achieve maximum degrees of freedom for the miso bc," available on arXiv:1211.4254, 2012.
- [18] X. Yi and D. Gesbert, "Precoding methods for the miso broadcast channel with delayed csit," *Wireless Communications, IEEE Transactions on*, vol. 12, pp. 1–11, May 2013.
- [19] P. de Kerret, X. Yi, and D. Gesbert, "On the degrees of freedom of the K-user time correlated broadcast channel with delayed CSIT," in *ISIT 2013, IEEE International Symposium on Information Theory, July 7-12, 2013, Istanbul, TURKEY*, July 2013. [Online]. Available: <http://www.eurecom.fr/publication/4000>
- [20] J. Chen, R. Knopp, and P. Elia, "Interference alignment for achieving both full dof and full diversity in the broadcast channel with delayed csit," in *Information Theory Proceedings (ISIT), 2012 IEEE International Symposium on*, Cambridge, MA, USA, 2012, pp. 1887–1891.
- [21] P. de Kerret and D. Gesbert, "Degrees of freedom of the network mimo channel with distributed csi," *IEEE Trans. on Info. Theory*, vol. 58, pp. 6806–6824, Nov. 2012.
- [22] B. Clerckx and C. Oestges, *MIMO Wireless Networks, 2nd Edition*. Academic Press, 2013.
- [23] C. Hao and B. Clerckx, "Imperfect and unmatched csit is still useful for the frequency correlated miso broadcast channel," in *IEEE ICC 2013*, Budapest, Hungary, Jun. 2013, available on arXiv:1302.6521.
- [24] J. Chen and P. Elia, "Optimal dof region of the two-user miso-bc with general alternating csit," available on arXiv:1303.4352, 2013.
- [25] C. Hao and B. Clerckx, "Miso broadcast channel with imperfect and (un)matched csit in the frequency domain: Dof region and transmission strategies," in *IEEE International Symposium on Personal, Indoor and Mobile Radio Communications (PIMRC) 2013*, London, United Kingdom, Sept. 2013.
- [26] C. Nair and A. El Gamal, "An outer bound to the capacity region of the broadcast channel," in *2006 IEEE International Symposium on Info. Theory*, Seattle, WA, 2006, pp. 2205–2209.
- [27] T. Liu and P. Viswanath, "An extremal inequality motivated by multiterminal information-theoretic problems," *IEEE Trans. Inf. Theory*, vol. 53, pp. 1839–1851, May 2007.
- [28] G. Caire, N. Jindal, M. Kobayashi, and N. Ravindran, "Multiuser mimo achievable rates with downlink training and channel state feedback," *Information Theory, IEEE Transactions on*, vol. 56, no. 6, pp. 2845–2866, June 2010.
- [29] T. M. Cover and J. A. Thomas, *Elements of Information Theory, second edition*. New York: Wiley-Interscience, 2006.

- [30] A. E. Gamal and Y.-H. Kim, *Network Information Theory*. Cambridge University Press, 2012.
- [31] A. Lapidath, S. Shamai, and M. A. Wigger, "On the capacity of fading mimo broadcast channels with imperfect transmitter side-information," available on arXiv: 0605079, 2006.
- [32] K. Marton, "A coding theorem for the discrete memoryless broadcast channel," *IEEE Trans. Inf. Theory*, vol. 25, pp. 306–311, Mar. 1979.